EPA-600/2-76-192
July 1976

Environmental Protection Technology Series

FILTRATION CHARACTERISTICS OF GLASS FIBER FILTER MEDIA AT ELEVATED TEMPERATURES

Environmental Sciences Research Laboratory
Office of Research and Development
U.S. Environmental Protection Agency
Research Triangle Park, North Carolina 27711

RESEARCH REPORTING SERIES

Research reports of the Office of Research and Development, U.S. Environmental Protection Agency, have been grouped into five series. These five broad categories were established to facilitate further development and application of environmental technology. Elimination of traditional grouping was consciously planned to foster technology transfer and a maximum interface in related fields. The five series are:

1. Environmental Health Effects Research
2. Environmental Protection Technology
3. Ecological Research
4. Environmental Monitoring
5. Socioeconomic Environmental Studies

This report has been assigned to the ENVIRONMENTAL PROTECTION TECHNOLOGY series. This series describes research performed to develop and demonstrate instrumentation, equipment, and methodology to repair or prevent environmental degradation from point and non-point sources of pollution. This work provides the new or improved technology required for the control and treatment of pollution sources to meet environmental quality standards.

This document is available to the public through the National Technical Information Service, Springfield, Virginia 22161.

EPA-600/2-76-192
July 1976

FILTRATION CHARACTERISTICS OF GLASS FIBER FILTER MEDIA AT ELEVATED TEMPERATURES

by

Dale A. Lundgren and Thomas C. Gunderson
Department of Environmental Engineering Sciences
University of Florida
Gainesville, Florida 32611

Grant No. 803126-01-0

Project Officer

Dr. Kenneth T. Knapp
Emissions Measurement and Characterization Division
Environmental Sciences Research Laboratory
Research Triangle Park, NC 27711

ENVIRONMENTAL SCIENCES RESEARCH LABORATORY
OFFICE OF RESEARCH AND DEVELOPMENT
U. S. ENVIRONMENTAL PROTECTION AGENCY
RESEARCH TRIANGLE PARK, NC 27711

DISCLAIMER

This report has been reviewed by the Environmental Sciences Research Laboratory, U.S. Environmental Protection Agency, and approved for publication. Approval does not signify that the contents necessarily reflect the views and policies of the U.S. Environmental Protection Agency, nor does mention of trade names or commerical products constitute endorsement or recommendation for use.

ABSTRACT

Particle collection characteristics of a newly developed, high-purity "Microquartz" fiber filter media and a Gelman Type A glass fiber filter media were evaluated over a range of temperatures 20°C to 540°C (68°F to 1004°F), particle sizes 0.05 μm to 26 μm, gas velocities 0.5 cm/sec to 51 cm/sec, and particle volatilities. Both types of high efficiency filters proved adequate (>99.9% efficiency) for sampling nonvolatile particles over the above variable ranges. Nonvolatile particle penetration decreased with increasing temperature and increasing filter loading.

The effect elevated temperature had on particle collection characteristics was not a determining factor in application of high efficiency filters. The main problems encountered in the high temperature environment were filter holder leakage and volatilization of gas-borne particles which passed through the filter media.

CONTENTS

TABLES

FIGURES

I. GENERAL INTRODUCTION

Glass fiber filter media is widely used for the collection of particulate matter from stack effluents. This filtration media is both inexpensive and highly efficient. It does, however, have a fairly high and variable background of extractable impurities, which often interferes with chemical analysis of collected particulate matter. To overcome this problem of a high extractable background, EPA supported development of a high-purity filter media made from Johns-Manville 99.2% "Microquartz" fibers. This development project, performed by A. D. Little, Inc.[1], produced a filter with a low extractable background suitable for stack gas sampling at temperatures in excess of 500°C (932°F).

When hot stack gases are sampled with EPA Method 5 sampling train[2], a significant fraction of what may be considered particulate matter is often found in the impingers downstream from the filter. The efficiency of glass fiber filter media has, therefore, been questioned. Furthermore, doubts about the effect of high temperature on filter performance and about filter efficiency for volatile particles have arisen. To answer these questions EPA supported this program to evaluate glass fiber filters, particularly the "Microquartz" filter, over a reasonable range of temperatures, velocities, particle sizes, and particle volatilities:

Temperature Range:	20°C to 540°C (68°F to 1004°F)
Velocity Range:	0.5 cm/sec to 51 cm/sec (≃1 ft/min to 100 ft/min)
Particle Diameter Range:	0.05 μm to 26 μm
Particle Composition:	Volatile and Nonvolatile

II. LITERATURE REVIEW: FILTRATION OF NONVOLATILE AEROSOLS

A. Theory

1. Introduction

The three factors which affect nonvolatile aerosol filtration are the dispersed particles, dispersing gas, and fibrous filter. Characterizing the dispersed particles are their size or size distribution, shape, mass, electrical charge, and concentration. Characterizing the dispersing gas are its velocity, density, absolute temperature, pressure, viscosity, moisture content, and composition. Finally, the fibrous filter is characterized by its surface area, thickness, fiber size or distribution of fiber sizes, filter porosity, specific fiber surface area, fiber composition, electrical charge, and surface characteristics.

Two phases may be distinguished in the filtration process—the primary phase and the secondary phase. In the primary phase, aerodynamic capture of particles occurs in a clean filter, so the following assumptions are usually made for models of this phase:

a) Deposition of individual particles does not influence filter efficiency.

b) Filter efficiency is time independent.

c) Any particle that touches a filter fiber is retained.

d) Particles are spherical.

e) All fibers have the same diameter.

f) Filter porosity is uniform.

g) Electrostatic, thermal, and gravitational effects are negligible.

h) No phase transitions occur in the aerosol during temperature changes.

In the secondary filtration phase, structural changes occur as a result of particle deposition; therefore efficiency is time dependent. So-called "secondary effects"[3] appear, consisting of deposition of particles upon one another, dendrite formation, fusion and flushing of drops on the fiber surfaces, capillary effects, loss of electrical charge, clogging, and so on.

The solution to the basic problem of predicting filtration efficiency is easier when regarded from the point of view of the first phase. Relatively good results have been obtained using primary phase assumptions, while published work including "secondary effects" has been empirical in nature. The section which follows discusses the basic collection mechanisms from the primary phase viewpoint approach.

2. Filtration Efficiency Equations

Aerosol filtration by fiber filters involves the three main collection mechanisms of diffusion, direct interception, and inertial impaction.[4] Diffusive capture of

particles is described by the dimensionless parameter N_D:

$$N_D = \bar{D}/DV \qquad [1]$$

where N_D = Dimensionless diffusion parameter

$\bar{D}$ = Diffusivity

D = Fiber diameter

V = Filtration velocity

Particle diffusivity is so related to absolute temperature and several other temperature dependent terms, that diffusive capture increases with increasing temperature (particularly for submicron particles). The following equations represent these relations:

$$\bar{D} = CkT/3\pi\eta d \qquad [2]$$

where $\bar{D}$ = Diffusivity

C = Cunningham correction factor

k = Boltzmann's constant

T = Absolute temperature

η = Gas viscosity

d = Particle diameter

$$C = 1 + (\lambda/d)[2.514 + (0.8)\exp(-0.55d/\lambda)] \qquad [3]$$

where C = Cunningham correction factor

λ = Mean free path of gas molecules

d = Particle diameter

$$\lambda = \eta/(0.499\rho_G c) \quad [4]$$

where λ = Mean free path of gas molecules

η = Gas viscosity

ρ_G = Gas density

c = Average velocity of gas molecules

$$\eta = \eta_o[(273.1 + G)/(T + G)](T/273.1)^{1.5} \quad [5]$$

where η = Gas viscosity at temperature T

η_o = Gas viscosity at temperature 0°C

T = Absolute temperature, °K

G = Constant = 114 for air at 1 atm

$$\rho_G = 1.293 \times 10^{-3}/[(1 + 3.67 \times 10^{-3})H] \quad [6]$$

where ρ_G = Air density, gm/cm

H = Temperature, °C

$$c = (8RT/\pi M)^{0.5} \quad [7]$$

where c = Average velocity of gas molecules

R = Universal gas constant

T = Absolute temperature

M = Gas molecular weight

Direct interception is defined by the temperature independent parameter N_R:

$$N_R = d/D \quad [8]$$

where N_R = Dimensionless interception parameter

d = Particle diameter

D = Fiber diameter

Inertial impaction is described by the Stokes' number:

$$STK = C\rho_p d^2 V/18\eta D \qquad [9]$$

where STK = Stokes' number
C = Cunningham correction factor
P_p = Particle density
d = Particle diameter
V = Filtration velocity
η = Gas viscosity
D = Filter diameter

Gas viscosity is the factor most affected by increasing temperature, rising with it. Hence, effectiveness of inertial impaction as a collection mechanism decreases with increasing temperature.

Efficiency of a filter mat is a function of N_R, N_D, and STK and is usually calculated from collection efficiency of the individual fibers comprising the mat. Many individual equations have been developed and recently were reviewed by Yeh.[7] One representative equation by Davies[8] is:

$$E_s = (0.16 + 10.9\alpha - 17\alpha^2)[N_R + (0.5 + 0.8N_R)(N_R + STK) - 0.105N_R(N_D + STK)^2] \qquad [10]$$

where E_s = Single fiber efficiency for diffusion, interception and inertial impaction
N_R = Dimensionless parameter for interception
N_D = Dimensionless parameter for diffusion

STK = Stokes' number

α = Packing density = $W/L\rho_F$

W = Mass per filter face area

L = Filter thickness

ρ_F = Fiber density

Filter mat efficiency can then be related to individual fiber efficiency by the following equation[9]:

$$E_M = 1-\exp[-4E_S W/\pi\rho_F D] \qquad [11]$$

where E_M = Filter mat efficiency

E_S = Single fiber efficiency for diffusion, interception, and inertial impaction [10]

W = Mass per filter face area

ρ_F = Fiber density

D = Fiber diameter

3. Secondary Processes in Aerosol Filtration

Filtration efficiency theories so far discussed are based on particle capture by clean fibers. Actually, a deposit builds up which may reduce the filter pore size and increase filter pressure drop. Often, deposited particles do not distribute themselves evenly over the surface of the fibers, but form chain aggregates which act as collection bodies and may capture particles more effectively than the filter itself. This process has been described by Watson[10] and Leers[11] and is illustrated in Figure 1.

Time variation of penetration and pressure drop of

a filter during use depends upon the filter structure, fiber shape, and nature of the aerosol. Several investigators, including Radushkevich,[3] have suggested that penetration descreases exponentially with time according to the equation:

$$P = P_o e^{-bt} \qquad [12]$$

where P = Penetration at time t=t

P_o = Penetration at time t=0

b = Constant under given conditions

4. Summary

The filtration theory presented explains the temperature effect on filter efficiency, which is defined as efficiency dependence on temperature of the filtered gas while all other conditions remain constant. However, the theory rests on very limiting assumptions (Section IIA1), which do not always hold, and does not allow for any "secondary effects." Nevertheless, filtration theory does illustrate both qualitatively and quantitatively that with only temperature increasing Figure 2):

1. Inertial deposition decreases due to the increase in gas viscosity.
2. Direct interception is essentially indenpendent of temperature.
3. Diffuse deposition increases due to greater particle diffusivity at higher temperatures (particularly for submicron particles).

B. Experimental Data of Others

First et al.[14] measured the efficiency of ceramic fiber filters [capable of withstanding temperatures up to 1093°C (2000°F)] at temperatures of 21°C (70°F) and 760°C (1400°F). Values of E_M = 85% at 21°C (70°F) and E_M = 82% at 760°C (1400°F) for fibers with a D = 20 μm were determined. For D = 8 μm, the corresponding values were E_M = 98% and E_M = 91%. For all experiments, the same conditions [d = 1 μm, V = 178 cm/sec, ρ_p = 6.4 g/cm^3] were maintained to keep the inertial mechanism of particle deposition dominant. The efficiency decreased for the three filters with increasing temperatures as predicted by theory.

Pich and Binek[13] reported measurements of temperature characteristics of a filter with D = 1.2 μm from 20°C (70°F) to 200°C (392°F)(Figure 3). NaCl cubic particles with each edge 0.2 μm and ρ_p = 2.16 g/cm^3 at V = 0.6 cm/sec were used. Under these conditions, diffusion deposition predominated, and efficiency increased from 94% [20°C (70°F)] to 98.5% [200°C (392°F)], reflecting filtration theory.

Dyment[15] reported results of some glass fiber filter tests with NaCl aerosol at temperatures up to 500°C (932°F). He found glass paper shrinks at these temperatures, so he

preheated the samples to avoid cracking. His paper does not mention D, d, ρ_p, and V. However, at ambient temperature, he found penetration too low (<0.001%) to be registered. The temperature was gradually raised to 440°C (824°F) when a penetration of 0.001% was measured. At 520°C (968°F) this increased to 0.09%. His conclusions were as follows:

"In practice the effect of temperature and pressure on filtration mechanism and performance has not been found a determining factor in the application of high efficiency filters. The main problems are the physical and chemical effects of a high temperature environment on the materials of construction of the filter which are manifested by reduced mechanical strength and resilience of loss of adhesion, leading to mechanical leakage and loss in efficiency."

More recent high temperature filter efficiency tests were reported by First.[16] Heat-shrunk quartz fiber filters were tested at temperatures up to 510°C (950°F) with a polydisperse NaCl aerosol of 0.14μm mass median diameter (mmd) at velocities (V) of 15 cm/sec to 30 cm/sec. Average penetrations ranged from 0.032% to 0.078% with no consistent trend with respect to temperature. Individual readings of NaCl penetration varied as much as ± 50% about the mean during each test series on an identical filter, so a trend would be difficult to detect.

Thring and Strauss[17] carried out filter efficiency calculations for a filter with D = 10μm, V = 25 cm/sec, and a temperature range of 0°C (32°F) to 1600°C (2912°F). Results for d = 0.01μm, d = 0.1μm, d = 5μm (Figure 4) show effect of temperature on inertial impaction, interception, and diffusion collection mechanisms.

III. LITERATURE REVIEW: FILTRATION OF H_2SO_4 AEROSOLS

A. Theory

1. Introduction

A major problem in stack sampling is how to classify gases at duct condition which condense and/or react in the filtering train and medium to form what may be considered particulate matter. One substance which falls into this category is sulfur trioxide (SO_3), formed in equilibrium with sulfur dioxide (SO_2) when sulfur-containing fossil fuels are burned. Up to 5% of the total sulfur in the fuel is converted to SO_3, yielding from 5 to 50 ppm SO_3 in the flue gas.[18,19] The SO_3 is in equilibrium with water (H_2O) vapor in the flue gas and, depending on temperature and gas component concentrations, various amounts of sulfuric acid (H_2SO_4) vapor will be formed. This H_2SO_4 can be collected on filters and weighed as particulate.

The importance of establishing whether or not condensed SO_3/H_2SO_4 is to be considered particulate matter is pointed out by a 36% average contribution of this material to total measured particulate grain loading (oil-fired boiler emissions) as reported by Jaworowski.[20] As fly ash emission levels are reduced by air pollution control equipment, this amount of condensed SO_3/H_2SO_4 may equal or surpass dry particulate contribution and could prevent compliance under existing regulations.

2. SO_x, H_2O and H_2SO_4 Equilibria in Flue Gas

Most sulfur in power plant flue gases appears as SO_2 (Table 1),[21] with typical SO_3 levels ranging from 1.0% to 2.5% of the SO_2. However, as Figure 5 shows, the equilibrium constant for the reaction:

$$SO_2 + 1/2\ O_2 \rightleftarrows SO_3$$

strongly favors the formation of SO_3 at temperatures below about 540°C (1000°F). This graph was calculated from data cited by Hedley.[22] Kinetics of the reaction are unfavorable in the absence of a catalyst, but thermodynamically the SO_3 concentrations could exist at levels much greater than those normally encountered. Ratios of SO_3 to SO_2 as high as 0.1 have been reported.[23] Since formation of SO_3 is controlled by catalytic effects as well as amount of excess air present, concentration of SO_3 resulting from combustion of a particular fuel can only be estimated in absence of direct measurements.

Reaction between H_2O vapor and SO_3 is given by:

$$H_2O + SO_3 \rightleftarrows H_2SO_4.$$

Figure 6 shows equilibrium conversion of SO_3 to H_2SO_4 as a function of temperature for a typical flue gas H_2O vapor concentration of 8 vol%. Appendix A illustrates the calculation method used in obtaining this curve. At temperatures below 204°C (400°F), essentially all SO_3 present is converted to H_2SO_4 at equilibrium. In contrast

to formation of SO_3, formation of H_2SO_4 occurs rapidly in the thermodynamically feasible temperature range.[24]

3. Determination of H_2SO_4 Dewpoint

Fly ash particles can influence the apparent dewpoint (saturation temperature of H_2SO_4 in flue gas), but one commits practically no error by neglecting the presence of other gases and considering only the H_2SO_4-H_2O system.[25] Thermodynamic analysis of the H_2SO_4-H_2O-flue gas system, ignoring fly ash effects, provides a theoretical basis for predicting acid dewpoints and condensate composition from vapor-liquid equilibria data.

Abel[26] was the first to derive a relationship enabling calculation of H_2SO_4, H_2O and SO_3 partial pressures from enthalpy, entropy, free energy, and heat capacity values. From his H_2SO_4 partial pressures and Greenwalt's H_2O partial pressures over H_2SO_4 solutions, H_2SO_4-H_2O dewpoint charts were prepared, Figures 7 and 8 . The range of uncertainty indicated by Abel is on the order of 5°C (9°F) at 10 vol% H_2O vapor.

Information contained in Figure 7 can be used to predict dewpoint temperature from an analysis of H_2SO_4 and H_2O vapor content. If gas is cooled below its dewpoint, condensate equilibrium concentration and mass can be obtained. Condensate mass predicted from use of the dewpoint chart is actually a prediction of the amount <u>available</u> for condensation. The <u>actual</u> amount of condensate depositing

on a fiber or metal surface may differ from the chart prediction because of mass transfer considerations.

As an example of the use of the chart, consider a flue gas containing 10 ppm H_2SO_4 and 10 vol% H_2O vapor. Condensation would occur at about 135°C (275°F), and condensate composition at that point would be about 79 wt% H_2SO_4. If the gas were cooled to 121°C (250°F), 85% of the H_2SO_4 would be removed from the gas phase and an insignificant amount of H_2O vapor would also condense. Condensation, therefore, follows the 10 vol% water line, resulting in a condensate which would be the equilibrium composition of the condensate at 121°C (250°F), assuming the vapor phase is in equilibrium with the total liquid condensed. Composition change of the liquid is small over the temperature interval given in this example, ranging from 79 vol% at 135°C (275°F) to 75 vol% at 121°C (250°F).

Large changes in H_2O vapor content of flue gases cause only slight changes in acid dewpoint. Variation of dewpoint with H_2SO_4 content of gases having different H_2O vapor concentrations is shown in Figure 9, where the range from 0.5 vol% to 15 vol% H_2O vapor changes dewpoint only 17°C (30°F) to 22°C (40°F) for the medium-to-high acid concentrations indicated.

In addition to the procedure based on calculated partial pressure, a number of efforts have been made to determine H_2SO_4 dewpoints from instrumental and chemical procedures. Figures 10 and 11 present results obtained for flue gas dewpoints as a function of H_2SO_4 content by various

investigators. To make an exact comparison, all curves should be for a gas of the same vol% H_2O vapor. However, reference to Figure 7 will indicate that a variation in H_2O vapor concentration from 7 vol% to 10 vol% can cause only about 1°C (2°F) to 2°C (4°F) change in dewpoint. Taylor's [29] results were obtained from an electrical dewpoint meter which is inaccurate at low acid partial pressures. Lisle and Sensenbaugh's[30] data were obtained with a spiral condenser. Dewpoint curves of Gmitro,[31] Muller,[25] Abel[26] and Greenewalt[27] were based on calculated partial pressures.

In view of the difficulties with calculation based on liquid phase thermodynamic properties and inaccuracy of dewpoint meters at low acid partial pressure, the most reliable method of correlating H_2SO_4 dewpoints with H_2O and H_2SO_4 vapor concentration is the experimental condensation method employed by Lisle and Sensenbaugh. Their data correlate best with Muller's calculated dewpoints and are the basis for ASME Power Test Code 19.10.

Rendle and Wilsdon[32] have also published some data on relation of the SO_3 content of combustion gas and of gas dewpoint to sulfur content of fuel oils, Figure 12 . Results of several other investigators have also been plotted. The type of oil, ash content, and combustion conditions differ for the various sets of points. Although the plot of SO_3 content shows considerable scatter, it is apparent that with more than 0.5% sulfur in the oil, SO_3 content of the gas does not increase proportionately to the fuel sulfur %.

Figure 12 indicates the following:

1. There is a rapid initial rise in dewpoint with the first increment of sulfur in the fuel. For an estimated dewpoint of 38°C (100°F) with no sulfur, an increase to 127°C (260°) (H_2SO_4 dewpoint) is found with 1% sulfur.

2. There is a relatively small rise in dewpoint as sulfur in the fuel oil increases from 1% to 6%.

B. Experimental Data of Others

Hillenbrand et al.[21] sampled flue gas from a coal-fired boiler with quartz filters maintained at 205°C (400°F) and 138°C (280°F) and found that filter temperature significantly affected the amount of H_2SO_4 found on the filter. At 138°C (280°F), 45% and 41% of the total H_2SO_4 catch (total H_2SO_4 mass in probe, filter, and impingers) were found on the filter in two trials. At 205°C (400°F), 24% and 8% of the total H_2SO_4 catch were found on the filter in two trials. The greater amount of H_2SO_4 found on the cooler filter was interpreted by them to mean:

1. A considerable portion of H_2SO_4 collected on the filter resulted from both condensation and reaction of particulate with the SO_2 and SO_3.

2. Condensation and consequent reaction is favored at lower temperature.

Jaworowski[20] sampled flue gas from several oil-fired

boilers with three different sampling methods: EPA Method 5 sampling train, ceramic thimble apparatus, and a high-volume sampling system. In all three sampling methods, temperature of the filter was kept between 120°C (250°F) and 150°C (300°F). His results (Table 2) show the magnitude of H_2SO_4 contribution to total particulate grain loading ranged from 18% to 78%, and averaged 36% of the total measured emissions.

IV. DESCRIPTION OF EXPERIMENTAL APPARATUS AND METHODS

A. General Experimental Arrangement

The experimental apparatus provided capabilities for: controlled aerosol generation, filter efficiency measurement (by fluorescent, gravimetric, atomic absorption, titrametric or microscopic counting techniques) and aerosol size distribution determination.

1. Nonacid Aerosols

The general arrangement of the experimental equipment is shown in Figure 13. Air was supplied from the building's compressed air system, filtered, and the stream split: one portion was used to operate an aerosol generator and the other to flow through an ion generator. The ion generator produced a high concentration of ions to accelerate attainment of a Boltzmann charge distribution on the aerosol in the conditioning chamber. Part of the aerosol leaving the conditioning chamber was exhausted and part heated in a stainless steel coil located in an oven. Aerosol temperature was measured with an iron-constantan (Type J) thermocouple, whose output was registered on a potentiometer (an ice point reference juction was used with the thermocouple). The heated aerosol then was split into two equal streams. The reference stream was piped out of the oven and consecutively through a coil immersed in cooling water, a high efficiency

particulate filter, a volumetric gas meter, a flow regulating valve, and a vacuum pump. The test stream first passed through the test filter, also in the oven, and then followed a route identical to that of the reference stream. Test filter efficiency was determined by using fluorescent, gravimetric, titrametric, and microscopic counting or atomic absorption techniques, depending on the type of test aerosol, to compare collected aerosol masses on the reference filter and backup filter following the test filter.

2. H_2SO_4 Aerosols

A special sampling train was used to experiment with H_2SO_4 aerosol. The train consisted of a heated box, to keep a stainless steel coil and test filter at the desired temperature; two Greenburg-Smith impingers filled with 100 ml of 80% isopropanol - 20% deionized water and immersed in an ice bath (to collect any H_2SO_4 that passed through the test filter); a backup filter to catch any carry-over mist from the impingers; a gas volumetric meter; a flow regulating valve; and a vacuum pump. Details of how H_2SO_4 was generated are in the next section.

B. Aerosol Generation

1. The Collison Atomizer

A Collison atomizer, as described by Green[36] and Whitby et al.[37-39] was used to generate aerosols in the 0.05 μm to 0.14 μm mmd range. The atomizer was operated at 2.1 kg/cm^2 (30 psig) pressure, which produced an 11 ℓ/min aerosol stream with ≃3 μm mmd particles. Flow was increased to 76 ℓ/min. upon dilution by the charge neutralizing stream from the ion generator. Placing an external impactor with a cut size of ≃ 2 μm in the line reduced particle size to about 1 μm mmd.

Solute-solvent combinations of uranine in distilled water and dinonyl phthalate in ethanol were used in the Collison atomizer. If generated droplets contained a dissolved solute, then upon evaporation, the diameter of the aerosol is:

$$d = \overline{C}^{1/3} D_d \qquad [13]$$

Whrre: d = Particle diameter

$\overline{C}$ = Ratio of solute volume to solvent volume plus solute volume

D_d = Droplet original diameter

Thus, an 8 vol % solution nebulized with a mean droplet diameter of 1 μm would produce a mean particle diameter of 0.43 μm.

Aerosol particles resulting from evaporation of the liquid phase sometimes carried significant excess static charge, which was effectively and quickly reduced by contact with a stream of bipolar ions.[37-39] The ionizer used to produce the ion stream was operated at 3000 volts A.C. with an air flow of 61 ℓ/min. A conditioning chamber of approximately 60ℓ capacity allowed achievement of an equilibrium charge distribution. Effectiveness of charge reduction was easily observed by measuring aerosol transmission loss in a short section of 0.63 cm O.D. Tygon tubing. For 0.14 μm mmd uranine aerosol flowing at 1 ℓ/min losses amounted to about 20% per meter without the ionizer and less than 5% per meter with it.

2. Spinning Disk Aerosol Generator

A spinning disk aerosol generator [36-38] was used to generate aerosols in the 0.5 μm to 6.0 μm mmd range. The disk's air motor speed, ionizer voltage, satellite air flow, liquid feed rate, and all other variables were held constant to produce a main droplet diameter of about 35 μm. Equation 13 was again used to predict aerosol size. Different size aerosols were generated by varying only solute

concentration. Uranine ethanol was the solute-solvent combination for all aerosol sizes generated with the spinning disk.

3. H_2SO_4 Aerosol Generation

H_2SO_4 aerosol was generated by evaporating 0.10 N H_2SO_4 in a stainless steel coil located in a 370°C (618°F) oven. The H_2SO_4 solution was metered at a constant rate with a 50 ml syringe driven by a constant speed syringe drive. A constant flow of ambient air was metered into the coil used for evaporation of the H_2SO_4. It was essential to add the acid uniformly to prevent undue fluctuations in the gas composition.

4. Other Methods of Aerosol Generation

For particles greater than 6.0 μm, Paper Mulberry Pollen (≃ 13 μm mmd) and Ragweed Pollen (≃ 26 μm mmd) were mechanically dispersed near the inlet to the filters with a rubber squeeze bulb. Fly ash with a 5.6 μm mmd (σ_g = 2.09) was also dispersed with compressed air near the inlet to the filters.

C. Determination of Aerosol Size Distribution

An electrical aerosol size analyzer was used to measure aerosol size distribution in the 0.01 μm to 0.50 μm

diameter range. Details of its operating theory and use are given in two papers by Liu et al.,[40-41] and in Thermo-Systems Operating Service Manual.[42] Since the electrical aerosol size analyzer gave a number median diameter (nmd), the mmd was calculated from the usual formula:

$$\text{Log(mmd)} = \text{Log(nmd)} + 6.9\ (\log \sigma_g)^2 \qquad [14]$$

In this equation the standard geometric deviation (σ_g) was found by plotting particle size versus number data on logarithmic cumulative probability graph paper. Then σ_g is calculated from:

$$\sigma_g = \frac{\text{nmd at 84.1\% value}}{\text{nmd at 50.0\% value}} \qquad [15]$$

Aerosols larger than 0.50 μm diameter were sized with a photomicroscope with incident illumination, again from the above two equations to obtain mmd's.

D. Temperature and Velocity Measurements

Air stream temperature was measured with an iron-constantan (Type J) thermocouple, with an ice bath reference junction and a potentiometer to record the thermocouple millivolt output. Clean, filtered air was passed through the system until the thermocouple reached equilibrium, so its response time was of minimal concern.

Gas velocity through the filter was determined by recording trial time, gas volume, temperature, ambient atmospheric pressure, vacuum pressure of the two volumetric gas meters, and pressure drops across all three filters. Gas velocity at the elevated temperature was then calculated from the following equation based on the Ideal Gas Laws:

$$V_F = (Q_M\ T_F\ P_M)/(A_F\ T_M\ P_F) \qquad [16]$$

where: V_F = Velocity through filter at T

T_F = Temperature of air stream

T_M = Temperature of volumetric gas meter

P_M = Atmospheric pressure - vacuum pressure

P_F = Atmospheric pressure + filter(s) pressure drop(s)

A_F = Filter area

Q_M = Volume at T_M registered by volumetric gas meter.

E. Techniques to Determine Filter Efficiency

1. Fluorescence

Fluorometric analysis[43,44] was used for most of the efficiency determinations, because it has excellent sensitivity ($\simeq$ 0.5 $\mu g/\ell$) and is easy to use. The procedure followed to determine the % penetration of a test filter was:

a) Wash in distilled water and dry several Gelman Type A (47 mm) filters to reduce their fluorescence background to an average of 0.5 μg/ℓ.

b) Use these washed filters in the parallel filter arrangement previously described.

c) Soak the uranine aerosol laden filters in 20 ml distilled water for 12 hours to insure all the uranine goes into solution.

d) Analyze the uranine leachate in a fluorometer to determine the uranine concentration.

e) Calculate the % penetration:

$$\% \text{ Penetration} = \frac{\text{Uranine mass on backup filter}}{\text{Uranine mass on reference filter}} \times 100\% \qquad [17]$$

The fluorescence of the uranine decreased to about 75% of its original value when exposed to 260°C(500°F). However, since the decrease was the same for the reference line and the test line, it did not affect the results. Uranine was not used for temperatures over 260°C (500°F), since its fluorescence is greatly reduced at these temperatures.

2. Atomic Absorption

A NaCl aerosol was used in place of uranine for temperatures from 260°C (500°F) to 538°C (1000°F). First[45] has demonstrated that the vaporization of NaCl at temperatures

less than or about equal to 538°C (1000°F) does not represent a serious error in the determination of filter penetration, especially since any error is on the conservative side.

The NaCl leachates from the filters were analyzed with an atomic absorption spectrophotometer. The calibration and operating procedures for the instrument were carefully followed as decribed in the instruction manuals.[46,47] For Na the practical working sensitivity proved to be about 3.0 µg/ℓ, much poorer than the 0.5 µg/ℓ sensitivity of the uranine fluorometric analysis. Consequently, longer test runs were needed to accumulate enough Na on the backup filter for accurate analysis. Teflon filters (5 µm pore size) were used in the reference and backup filter holder because they had undetectable Na backgrounds. Gelman Type A, Gelman Spectro Grade Type A, and Millipore Membrane (0.8 µm pore size, white, 47 mm) filters all proved to have Na backgrounds too high to be useful.

3. Mass Measurement

For the dinonyl phthalate aerosol, penetrations at elevated temperatures were high enough for the aerosol to be detectedby its mass alone. By weighing the filters before and after the experimental runs, it was possible to determine the mass of accumulated aerosol. A microbalance with a sensitivity of 0.0001 g was used for the weighings.

4. Microscopic Counting

The larger pollen aerosols were easily visible under a stereo microscope, so penetrations could be determined by counting the individual pollen particles. Millipore Membrane Filters (0.8 μm pore size, black, 47 mm) were used as backups to collect the few pollen particles that penetrated the filter under test.

5. Titration

H_2SO_4 masses in washings of the stainless steel coil, leachates of the filters, and the impinger contents were determined by titration with 0.01 N NaOH. The NaOH titrant was standardized against 0.01 N potassium acid phthalate. Phenolphthalein indicator (0.05 wt % in deionized water) was used.

F. Filters and Filter Holders

Two types of glass fiber filters suitable for high temperature sampling were used as test filters. One was the binderless Gelman Type A Glass Fiber Filter (47 mm), manufactured from microsize filaments of glass and treated in a muffle furnace to remove trace amounts of organic fiber content. This filter is acceptable for use in EPA Method 5. It withstood 538°C (1000°F) but became brittle at that temperature. The other filter used was a

prototype "Microquartz" filter[1] of 99.2% silica fibers, by Johns-Manville Company. It maintained its structural strength and flexibility even at 538°C (1000°F).

Two filter holders with different effective filtering areas enabled the coverage of a wide velocity range of 0.50 cm/sec to 51.0 cm/sec. A stainless holder (Gelman No. 2220, 47 mm) was used for the higher velocities. Its effective filtration area was 9.6 cm^2, and its Viton O-ring and Teflon captive thrust ring proved capable of withstanding 260° C (500°F). Removing these two parts for higher temperatures did not cause the holder to leak. Two holes were drilled and tapped into the holder for threaded stainless steel capillary tubing for pressure taps. This holder style was also used to hold the reference and backup filters.

A 10 cm Pyrex glass filter holder with an effective filtration area of 64 cm^2 was used for the lower velocity range. The filter holder consisted of two glass halves, fritted glass filter backing, and a two-piece metal clamp with four bolts. The low melting point of the Neoprene gasket prevented the filter holder from being used above 260°C (500°F). Also, expansion of the bolts at 260°C (500°F) caused the holder to leak excessively (Section VF). Therefore, small springs were placed on each bolt between the locking nut and the metal clamp (Figure 14) to prevent leakage.

V. RESULTS AND ANALYSIS

Particle collection efficiency tests with Gelman Type A, Gelman Type E, Gelman Spectrograde Type A, Mine Safety Appliance Type 1106BH, and "Microquartz" glass fiber filters all produced very similar results at room temperature. These filter media all have similar pressure drops vs. flow rates filter masses per unit area, and fiber size distribution (see Appendices B and C). Therefore, only the Gelman Type A filter was extensively tested for comparison with the new "Microquartz" filter at high temperatures.

A. Aerosol Size Distribution

The aerosols generated with the Collison atomizer with impactor were sized with an electrical aerosol size analyzer. Their distributions (Table 3) were slightly more polydisperse than those of Liu[48] (Table 4), who used a more similar Collison-Impactor generator. The size distributions of the aerosols larger than 0.50 μm diameter were determined with a photomicroscope using incident illumination (Table 5).

B. Loading Effects on Filtration Efficiency

Penetration of both the Gelman Type A and Micro-

quartz filters declined significantly with aerosol loading of only several micrograms per square centimenter. This effect was noted at both 20°C (70°F) and 260°C (500°F) (Figure 15) and was accompanied by a filter-pressure-drop-increase of less than 5%. A test to determine if the uranine aerosol had an excessive charge which might have contributed to this phenomenon proved negative. If the filter was initially charged, the contribution to total filter efficiency (due to filter charge) should have dissipated with time as the charge was lost, thus increasing penetration. This did not happen. So, the penetration decrease was attributed to plugging of microsized holes by the first few micrograms of aerosol and/or tree-like branches formed by the initial aerosol deposit serving as particle collection surfaces. The latter proposition is supported by Tomaides'[49] findings that particles can form a rather sturdy bridge about 10 particle diameters long.

A similar increase in efficiency well before an appreciable filter-pressure-drop-increase was reported by Dorman.[50] He reported that a filter with an initial efficiency of 99.50% on a heterodisperse aerosol of 0.6 μm mmd had a final efficiency of 99.98%, while the filter pressure drop changed from 2.50 cm to 2.75 cm H_2O.

The time variation of penetration of a filter during use naturally depends on the filter structure, fiber

material and the nature of the aerosol. As previously discussed, Radushkevich suggested penetration decreases exponentially with time according to the equation:

$$P = P_0 e^{-bt} \qquad [18]$$

Where: P = Penetration at time t=t

P_0 = Penetration at time t=0

b = Constant under given conditions

From the data in Figure 15, the following b values were calculated:

Filter Type	t(min)	Temperature (°C)	b(min^{-1})
Type A	100	21 (70°F)	0.0233
Type A	180	260 (500°F)	0.008
"Microquartz"	100	21 (70°F)	0.0240
"Microquartz"	180	260 (500°F)	0.005

With these b values, plots on semi-log graph paper of $P=P_0e^{-bt}$ between the initial penetration and the final penetration measurements compared favorably with the experimental data.

To negate the decreasing penetration when comparing filter penetrations, two consecutive tests were run on each filter. The two measured penetrations were then plotted on the normal axis of semi-logarithmic graph paper (Figure 16), while the respective average loadings were plotted on the logarithmic axis. Penetration at the arbitrary reference

loading of 7 $\mu g/cm^2$ was then found by interpolation between the two test penetration values.

C. Velocity Effects on Filtration Efficiency

Penetration of submicron aerosols was found to increase with increasing velocity (Figures 17 and 18). Similar penetrations for the 0.09 μm mmd and 0.14 μm mmd aerosols were not expected but may indicate the presence of microsized holes in the filter media. Penetrations of less than 0.01% were found for aerosols greater than about 0.8 μm mmd for all filtration velocities tested. These penetrations were so low that the aerosol measurement sensitivity was inadequate to determine larger particle velocity effects on filter efficiency. This, in general, was also true for all particle sizes at filtration velocities of less than 5 cm/sec.

The filter pressure drops increased linearly with velocity (Figure 19), resembling the findings of Benson, et al., and obeying D'Arcy's Law:

$$\Delta p = XL\eta V \qquad [19]$$

Where Δp = Pressure drop

X = Permeability coefficient (a constant)

L = Filter thickness

η = Gas viscosity

V = Velocity

D. Effect of Particle Size on Filtration Efficiency

Submicron aerosols were found to produce the greatest filter penetrations (Figures 20 and 21). Similar penetrations for particles less than 0.14 μm mmd cannot be easily explained except for the possible presence of microsized holes. Uranine aerosols greater than 0.8 μm mmd, fly ash aerosol of 1.10 μm mmd, a dinonyl phthalate oil aerosol of about 1.0 μm mmd, and pollen aerosols of 13.1 μm and 26.7 μm mmd's all evidence penetrations of less than 0.01% at ambient temperatures.

E. Effect of Temperature on Filtration Efficiency

The effect of increased temperature was to decrease aerosol penetration for nonvolatile submicron particles whose penetration could be measured (Table 6 and Figure 22). Since submicron particles are collected mainly by diffusion, which is more effective with increasing temperature, the experiemental results qualitatively confirm the theory previously outlined.

Volatile particles were not collected as effectively at elevated temperatures as were the nonvolatile particles. For example, a Gelman Type A filter was tested at 21°C (70°F), 150°C (374°F), and 260°C (500°F) with a dinonyl phthalate (DNP) aerosol, which vaporizes at 232°C (450°F). The results at a 51 cm/sec filtration velocity

were:

Temp (°C)	%Penetration
20	< 0.01
150	≃ 25
260	≃100

Obviously,at 260°C (500°F) the DNP vaporized, passed through the filter, and condensed upon being cooled below its dew-point. DNP was found both in the cooling coil following the test filter and on the backup filter.

These results imply that the definition of particulate matter is a function of the sampling method (i.e., the temperature at which the sample is collected). Consequently, if compliance tests are to be compared from source to source, the same sampling method (i.e., sampling temperature) must be employed if volatiles or condensables are involved.

Filter pressure drop also increased with increasing temperature, due to the increasing air viscosity values at elevated temperatures. This effect (Figure 23) reflects D'Arcy's Law (Equation 19) in which pressure drop is directly proportional to both viscosity and velocity.

F. Filter Holder Leakage

A stainless steel filter holder (Gelman No. 2220, 47 mm)was used for most of the experiments and was air-tight at temperatures to 538°C (1000°F). However, a Pyrex glass filter holder held together by a two-piece metal clamp with

four bolts leaked significantly at 260°C (500°F). The metal bolts expanded, deforming the clamping device and creating a relatively large air leak. This resulted in an apparent 50% to 60% aerosol penetration. This leakage problem was corrected by spring loading the bolts of the metal clamp.

In EPA Method 5[2], a leakage check of the sampling train, including the filter holder, is usually done with the system at ambient temperature. From our findings, it would seem necessary to bring the filter unit to the recommended temperature of 120°C before making the leakage check. This precaution would become even more necessary if the proposed Method 5 filter box temperature maximum of 160°C (320°F)[51] is accepted.

G. H_2SO_4 Filtration Efficiency at Elevated Temperatures

Experiments with H_2SO_4 aerosol were conducted at two temperatures [120°C (248°F), 205°C (401°F)],25 cm/sec filtration velocity, 8.5 vol % H_2O vapor,and 140 ppm ($\pm$15 ppm) H_2SO_4. At these concentrations of H_2SO_4 and H_2O vapor, the acid dewpoint is about 170°C (338°F). The results in Table 7 show at 120°C (248°F), below the H_2SO_4 dewpoint, most of the H_2SO_4 was found in the coil and on the test filter. At 205°C (401°F), above the H_2SO_4 dewpoint, most of the H_2SO_4 was found after the test filter in the impinger contents and on the backup filter. Simple calculations based on typical stack sampling data from oil-

fired boilers and on this experimental data indicate H_2SO_4 could account for more than 50% of the total particulate catch at a 120°C (248°F) sampling temperature (or at a temperature below the H_2SO_4 dewpoint in the stack gas), but only for about 9% at a 205°C (401°F) sampling temperature (or at a temperature above the H_2SO_4 dewpoint in the stack gas).

H. Pinhole Effects on Filter Efficiency

Figure 24 shows how the penetration of a high efficiency glass fiber filter was affected by punching two 0.75 mm diameter pinholes through the filter mat. Note that penetration is greater for the small aerosol than for the large aerosol. The pinholes were clearly visible when the filter was examined against an illuminated background, so it is doubtful whether defective filters with pinholes as large as these would pass unnoticed and be used for sampling. These penetrations are small enough not to significantly affect the outcome of a stack sampling test.

I. Comparison of Theory with Experimental Data

Equations 10 and 11 were used to calculate the theoretical efficiency of the "Microquartz" filter, and the results are in Table 8. Both the theory and data show penetration to decrease with rising temperature. The theoretical penetrations are only within two orders of

magnitude of the experimental penetrations, being very dependent on the filter fiber diameter and particle size and/or size distribution. Work is presently being done by us to improve the accuracy of several theoretical filtration equations.

J. Experimental Errors

The largest variables in the experiments were the changes in penetration from filter to filter. As an illustration, the penetrations of ten Gelman Type A filters were tested under identical conditions [T=21°C (70°F), V=18 cm/sec, d=0.14μm mmd] using fluorometric analysis. The penetrations ranged from 0.02% to 0.05% at 7.0 $\mu g/cm^2$ loading; the average penetration was 0.03% $\pm$ 0.01%. Allowing for the sensitivity of the fluorometric analysis (0.5 μg/ℓ or 0.005% penetration for these trials), the filter-to-filter penetrations varied as much as 67% from the average penetration for the ten trials.

The atomic absorption analytic method which was used for the analysis of NaCl was not as sensitive as the fluorometric technique. The sensitivity of the former was 3.0 μg/ℓ, while that of the latter was 0.5 μg/ℓ. Hence, more mass had to be accumulated on the test filter so that enough aerosol penetrated to be detected accurately. The accuracy of the atomic absorption method was $\pm$ 0.01% penetration, which was adequate, considering the large variability from

filter to filter.

The smallest detectable H_2SO_4 mass, with titration of 0.01 N NaOH was about 45 µg. Since the H_2SO_4 mass collected in the impingers, coil, or filters was about 6,000µg, the error due to the titration was less than about 0.75%. However, completely flushing all the H_2SO_4 from inside the coil with deionized water was difficult, so about a ± 10% error in the H_2SO_4 masses determined for the coil can be assumed.

The accuracies of temperature and velocity measurements were ±10% and ±5% respectively. The sensitivity of the mass determinations, using a microbalance, was ±0.0002 g. This translates into an accuracy in penetration of ±0.67%. The mass method of determining filter efficiency was used only for the dinonyl pthalate aerosol, which penetrated 100% at some high temperature conditions. Thus, ±0.67% penetration was sufficient accuracy.

Due to the inherent errors in particle size measurement by electrical mobility, the mmd's determined with an electrical aerosol size analyzer were not better than ±20%. About the same accuracy can be ascribed to the size distributions made by counting the particles with a light microscope. The size of the aerosols generated with the Collison atomizer with impactor compared favorably with the size of those generated by others (See Tables 3 and 4).

VI CONCLUSIONS

It was experimentally demonstrated that Gelman Type A and "Microquartz" high efficiency glass fiber filters are adequate for sampling nonvolatile particles at temperatures to 538°C (1000°). Submicron particles penetrated more than did larger particles, and they penetrated the most at the highest filtration velocity tested (51 cm/sec). In all tests, however, the aerosol penetration was never more than about 0.10%. Nonvolatile particles penetrated less with increasing temperature and increasing filter loading.

Particles with vaporization points below the sampling temperature, including H_2SO_4, can vaporize, pass through the glass fiber filters, and then recondense when cooled below their dewpoints. Therefore, the definition of "particulate matter" must be based upon a prescribed temperature. Hot stack gases sampled at different filter temperatures should not necessarily be comparable. Particulate emission standards must involve a suitable reference temperature to allow proper enforcement.

Filtration efficiencies calculated by theoretical equations change dramatically with small changes in the assumed average filter fiber diameter and/or particle size (or size distribution) used in the calculations.

Pinholes not visible to the naked eye do not appear to affect the penetration of glass fiber filters enough to significantly alter stack sampling results.

The effect of temperature on filtration of non-volatile particles was an increase in the collection of submicron particles with increasing temperature. The main problems encountered at elevated temperatures were vaporization of volatile particles and mechanical leakage of the filter holder.

SYMBOLS

A_F = Filter area

b = Constant (In Equation 12)

$\overline{C}$ = Ratio of solute volume to solvent volume plus solute volume

C = Cunningham correction factor

c = Average velocity of gas molecules

d = Particle diameter

D_d = Droplet original diameter

D = Fiber diameter

$\overline{D}$ = Diffusivity

E_M = Filter mat efficiency

E_s = Single fiber efficiency for diffusion, interception and inertial impaction

G = Constant (In Equation 5)

H = Temperature, °C

k = Boltzmann's constant

L = Filter thickness

M = Molecular weight of gas

N_R = Dimensionless interception parameter

N_D = Dimensionless diffusion parameter

P = Penetration at time t = t

P_o = Penetration at time t = 0

Q_M = Volume at T_M registered by volumetric gas meter

R = Universal gas constant

STK = Stokes' number

T_M = Temperature of volumetric gas meter

T = Absolute temperature

T_F = Temperature of air stream

V = Filtration velocity

V_F = Velocity through filter at T_F

W = Mass per filter face area

X = Permeability coefficient

α = Packing density

Δp = Pressure drop

ρ_F = Fiber density

ρ_G = Gas density

ρ_p = Particle density

η = Gas viscosity

η_o = Gas viscosity at 0°C

λ = Mean free path of gas molecules

P_M = Atmospheric pressure - vacuum pressure

P_F = Atmospheric pressure + filter(s) pressure drop(s)

References

1. Benson, A. L., Levins, P. L., Massucco, A. A., and Valentine, J. R., Development of a High-Purity Filter for High Temperature Particulate Sampling and Analysis, EPA-650/2-73-032, by Arthur D. Little, Inc., Cambridge, Mass., Nov. 1973.

2. "EPA Standards of Performance for New Sources," Federal Register, 36 (247):24876 (1971).

3. Radushkevich, L. V., Izv. Akad. Nauk SSSR, ser. khim. nauk, 3:407 (1963).

4. Chen, C. Y., "Filtration of Aerosols by Fibrous Media," Chem. Rev., 55:595-623 (1955).

5. Perry, J. H., and Chilton, C. H., Chem. Engineer's Handbook, 5th Ed., McGraw Hill Book Co., Inc., New York, p. 3-248 (1973).

6. Hodgman, C. D., Handbook of Chemistry and Physics, Chemical Rubber Publishing Co., Cleveland, Ohio, p. 2205 (1962).

7. Yeh, H. C., A Fundamental Study of Aerosol Filtration by Fibrous Filters, Univ. of Minn., Ph.D. Thesis (1972).

8. Davies, C. N., "The Separation of Airborne Dust and Particles," Proc. Inst. Mech. Engng., 1B:185 (1952).

9. Whitby, K. T. and Lundgren, D. A., "Mechanics of Air Cleaning," Trans. of ASAE, 8(3):342-344, 351-352 (1965).

10. Watson, J. H. L., "Filmless Sample Mounting for the Electron Microscope," J. Appl. Phys., 17:121-127 (1946).

11. Leems, R., "Die Abscheidung Von Schwebstaffen in Fasernfiltern," Staub, 50:402-417 (1967).

12. Davies, C. N., Aerosol Science, Academic Press, New York, p. 270 (1966).

13. Pich, J., and Binek, B., "Temperature Characteristics of Fiber Filters," in Aerosols, Physical Chemistry and Applications, Proc. First Nat. Conference on Aerosols, p. 257-264, Czech. Akad. Sciences, Prague (1965).

14. First, M. W., Graham, J. B., Butler, G. M., Walworth, C. B., and Wanen, R. P., "High Temperature Dust Filtration," Ind. and Eng. Chem., 48(4):696-720 (1956).

15. Dyment, J., "Assessment of Air Filters at Elevated Temperatures and Pressures," Filtration and Separation, p. 441-445, July/August (1970).

16. First, M. W., "Performance of Absolute Filters at Temperatures from Ambient to 1000°F," 12th AEC Air Cleaning Conference, p. 677-702.

17. Thring, M. W., and Strauss, W., "The Effects of High Temperature on Particle Collection Mechanisms, "Trans. Instn. Chem. Engrs., 41:248-259 (1963).

18. Danielson, J. A., Air Pollution Engineering Manual, Los Angeles County Air Pollution Control District, Los Angeles, Cal., p. 536, 1967.

19. Hemeon, W. C. L., and Black, A. W. J., "Stack Dust Sampling: In-Stack Filter or EPA Train," J. Air Poll. Control Assoc., Vol. 22, No. 7, p. 516, 1972.

20. Jaworowski, R. J., "Condensed Sulfur: Trioxide Particulate or Vapor?" J. Air Poll. Control Assoc., Vol. 23, No. 9, p. 791, 1973.

21. Hillenbrand, L. J., Engdahl, R. B., and Barrett, R. E., Chemical Composition of Particulate Air Pollutants From Fossil-Fuel Combustion Sources, Battelle Columbus Laboratories, p. II-2, March 1, 1973.

22. Hedley, A. B., in The Mechanism of Corrosion by Fuel Impurities (H. R. Johnson and D. L. Littler, editors), Butterworth, London, p. 204, 1963.

23. Cuffe, S. T., Gerstle, R. W., Orning, A. A. and Schwartz, C. H., J. Air Poll. Control Assoc., Vol. 14, p. 353, 1964.

24. Snowden, P. N. and Ryan, M. H., "Sulfuric Acid Condensation from Flue Gases Containing Sulfur Oxides," J. Inst. Fuel, Vol. 42, p. 188, 1969.

25. Mueller, P., "Study of the Influence of Sulfuric Acid on the Dew Point Temperature of the Flue Gas," Chemie-Ing.-Tech., Vol 31, p. 345, 1959.

26. Abel, E., "The Vapor Phase Above the System Sulfuric Acid-Water," J. Phys. Chem., Vol. 50, p. 260, 1946.

27. Greenewalt, C. H., "Partial Pressure of Water Out of Aqueous Solutions of Sulfuric Acid," Ind. and Eng. Chem., Vol. 17, pp. 522-523.

28. Matty, R. E., and Diehl, E. K., "New Methods for Determining SO_2 and SO_3 in Flue Gas," Power Engineering, Vol. 57, p. 87, Dec., 1953.

29. Taylor, A. A., "Relation Between Dew Point and the Concentration of Sulfuric Acid in Flue Gases," J. Inst. Fuel, Vol. 16, p. 25, 1942.

30. Lisle, E. S. and Sensenbaugh, J. D., "The Determination of Sulfur Trioxide and Acid Dew Point in Flue Cases," Combustion, Vol. 36, No. 1, p. 12, 1965.

31. Gmitro, J. I., and Vermuelen, T., "Vapor-Liquid Equilibria for Aqueous Sulfuric Acid," Univ. of Cal. Radiation Lab. Report 10866, Berkeley, Cal., June 24, 1963.

32. Rendle, L. K., and Wilson, R. D., "The Prevention of Acid Condensation in Oil-Fired Boilers," J. Inst. Fuel, Vol. 29, pp. 372-380, 1956.

33. Taylor, R. P., and Lewis, A., "Sulfur Trioxide Formation in Oil Firing," Proc. Fourth Inst. Congress on Industrial Heating, Group II, Sec. 24, No. 154, Paris, France, 1952.

34. Flint, D., Lindsay, A. W., and Littlejohn, R. F., "The Effect of Metal Oxide Smokes on the SO_3 Content of Combustion Gases from Fuel Oils," J. Inst. Fuel, Vol. 26, pp. 122-127, 1953.

35. Corbett, P. F., and Fireday, F., "The SO_3 Content of the Combustion Gases from an Oil-Fired Water-Tube Boiler," J. Inst. Fuel, Vol. 26, pp. 92-106, 1953.

36. Green, H. L., and Lane, W. R., Particulate Clouds: Dusts Smokes and Mists, E. & F. M. Spon. Ltd., London, 1957.

37. Whitby, K. T., Lundgren, D. A., and Jordan, R. C., "Homogeneous Aerosol Generators," Technical Report No. 13, Cooperative Research Project, Univ. of Minn., Dept. of Mech. Eng. and USPHS (USPHS Grant No. S-23 (C-4), Jan., 1961.

38. Whitby, K. T., Lundgren, D. A., and Peterson, C. M., "Homogeneous Aerosol Generators," J. Air and Water Pollution, Vol. 9, p. 263, 1965.

39. Whitby, K. T., Generator for Producing High Concentrations of Small Ions," Rev. Sci. Inst., Vol. 32, p. 1351, 1961.

40. Liu, B. Y. H., and Pui, D. Y. H., "On the Performance of the Electrical Aerosol Analyzer," Particle Technology Lab. Publ. No. 237, Particle Tech. Lab., Mech. Eng. Dept., Univ. of Minn., Oct., 1974.

41. Liu, B. Y. H., Whitby, K. T., and Pui, D. Y. H., "A Portable Electrical Analyzer for Size Distribution Measurement of Submicron Aerosols," J. Air Poll. Control Assoc., Vol 24. No. 11, Nov., 1974, p. 1067.

42. TSI Model 3030 Electrical Aerosol Size Analyzer Operating and Service Manual, Thermo-Systems, Inc., St. Paul, Minn.

43. Manual of Fluorometric Clinical Procedures, G. K. Turner Assoc., Nov., 1971.

44. Operating and Service Manual Model 110 Fluorometer, G. K. Turner Assoc., April, 1971.

45. First, M. W., "Performance of Absolute Filters at Temperatures from Ambient to 1000°F," 12th AEC Air Cleaning Conference, pp. 677-702.

46. Instruction Manual for Models 1100 and 1200 Atomic Absorption Spectrophotometers, Varian Techtron Pty., Ltd., Melbourne, Australia, Sept., 1973.

47. Analytical Methods for Flame Spectroscopy, Varian Techtron Pty., Ltd., Melbourne, Australia, Sept., 1972.

48. Liu, B. Y. H., "Methods of Generating Monodisperse Aerosols," Pub. No. 104, Particle Technology Lab., Mech. Eng. Dept., Univ. of Minn., Feb. 8, 1967.

49. Tomaides, M., U. of Minn., Personal Communication (1967) in: Billings, C. E., Wilder, J., Fabric Filter Systems Study. Vol. I: Handbook of Fabric Filter Technology, GCA Corporation, Report No. NTIS No. PB 200-648, 1970, pp. 200-648, 1970, pp. 2-83.

50. Dorman, R. G., "Filtration," in Aerosol Science by C. N. Davies, Academic Press, N.Y., p. 218, 1966.

51. Federal Register, Vol. 39, No. 177, Sept. 11, 1974, p. 32853.

52. Yost, D. M. and Russell, H., Jr., Systematic Inorganic Chemistry, Prentice-Hall, Inc., N.Y., 336 pp. (1946).

APPENDIX A

CONVERSION OF SO_3 TO H_2SO_4

To answer the question of how much of the SO_3 in flue gas is present as H_2SO_4, consider the following equilibrium:[52]

$$H_2SO_4(g) \rightleftarrows SO_3(g) + H_2O(g)$$

$$K = \frac{(H_2O)(SO_3)}{(H_2SO_4)} \quad \text{(moles vapor/ℓ)}$$

$$\log_{10}K = \frac{-22850}{4.571T} + 0.75 \log_{10}T - 0.00057T + 4.086$$

(over the temperature range 598 to 756°K)

First calculate position of the above equilibrium at the highest temperature of interest, 400 F (477°K) assuming the above expression for $\log_{10}K$ is valid:

$$\log_{10}K = 10.480 + 2.009 - 0.272 + 4.086$$

$$= -4.657$$

so at 400°F $\quad K = 0.22 \times 10^{-4} = \frac{(H_2O)(SO_3)}{(H_2SO_4)}$

at 1 atm, 0°C, ideal gas $= \frac{1}{22.40}$ m/ℓ $= 0.0446$ m/ℓ

at 1 atm, 477°K ideal gas $= \frac{273}{(477)(22.40)} = 0.0256$ m/ℓ

In the typical exhaust-gas composition from a coal fired boiler (Table 1), $H_2O = 4\%$,

so $H_2O = 0.04 \times 0.0256 = 1.024 \times 10^{-3}$ m/ℓ.

Similarly, $SO_3 = (3.0 \times 10^{-5} \times 2.56 \times 10^{-2} - X) = (7.7 \times 10^{-7} - X)$ moles/ℓ

$H_2SO_4 = X$ moles/liter

$$0.220 \times 10^{-4} = \frac{(1.02 \times 10^{-3})(7.7 \times 10^{-7} - X)}{X}$$

$X = 7.51 \times 10^{-7}$; or 97.8% of the SO_3 is H_2SO_4.

Similarly, at 300 °F (422 °K):

$$\log_{10} K = 11.846 + 1.970 - 0.241 + 4.086$$

$$\log_{10} K = -6.031$$

$$K = 0.935 \times 10^{-6}$$

at 1 atm, 422 °K, ideal gas is $0.446 \times \frac{273}{422} = 0.289$ m/ℓ

$$H_2O = 0.40 \times 0.0289 = 1.16 \times 10^{-3} \text{ m/ℓ}$$

$$H_2SO_4 = X \text{ m/ℓ}$$

$$SO_3 = 3 \times 10^{-5} \times 0.0289 - X = (8.66 \times 10^{-7} - X) \text{ m/ℓ}$$

$$0.035 \times 10^{-6} = \frac{(1.16 \times 10^{-3})(8.66 \times 10^{-7} - X)}{X}$$

$$(0.935 \times 10^{-6})X = 1.04 \times 10^{-9} - (1.16 \times 10^{-3})X$$

$$X = \frac{1.004 \times 10^{-9}}{1.16 \times 10^{-3}} = 0.866 \times 10^{-6}$$

at 300 F $H_2SO_4 = 8.66 \times 10^{-7}$; or ≃ 100% of the SO_3 is H_2SO_4.

Hence, SO_3 essentially exists as H_2SO_4 over the entire range of conditions of interest, if the time is sufficient to allow equilibrium of the hydration.

(Above from Hillenbrand, *et al.*[21])

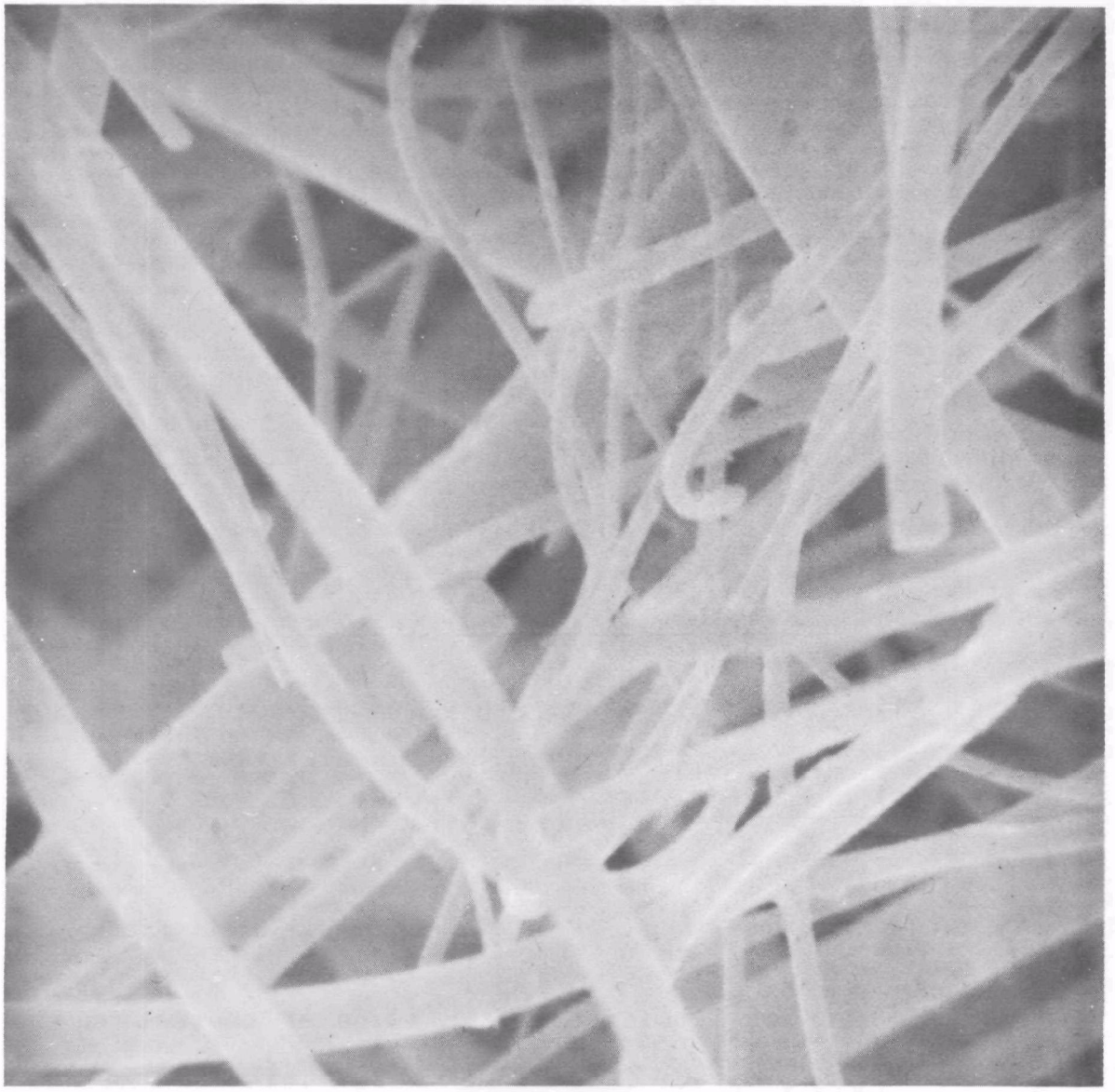

1 µm

"Microquartz" filter at 5000x magnification (scanning electron microscope photo).

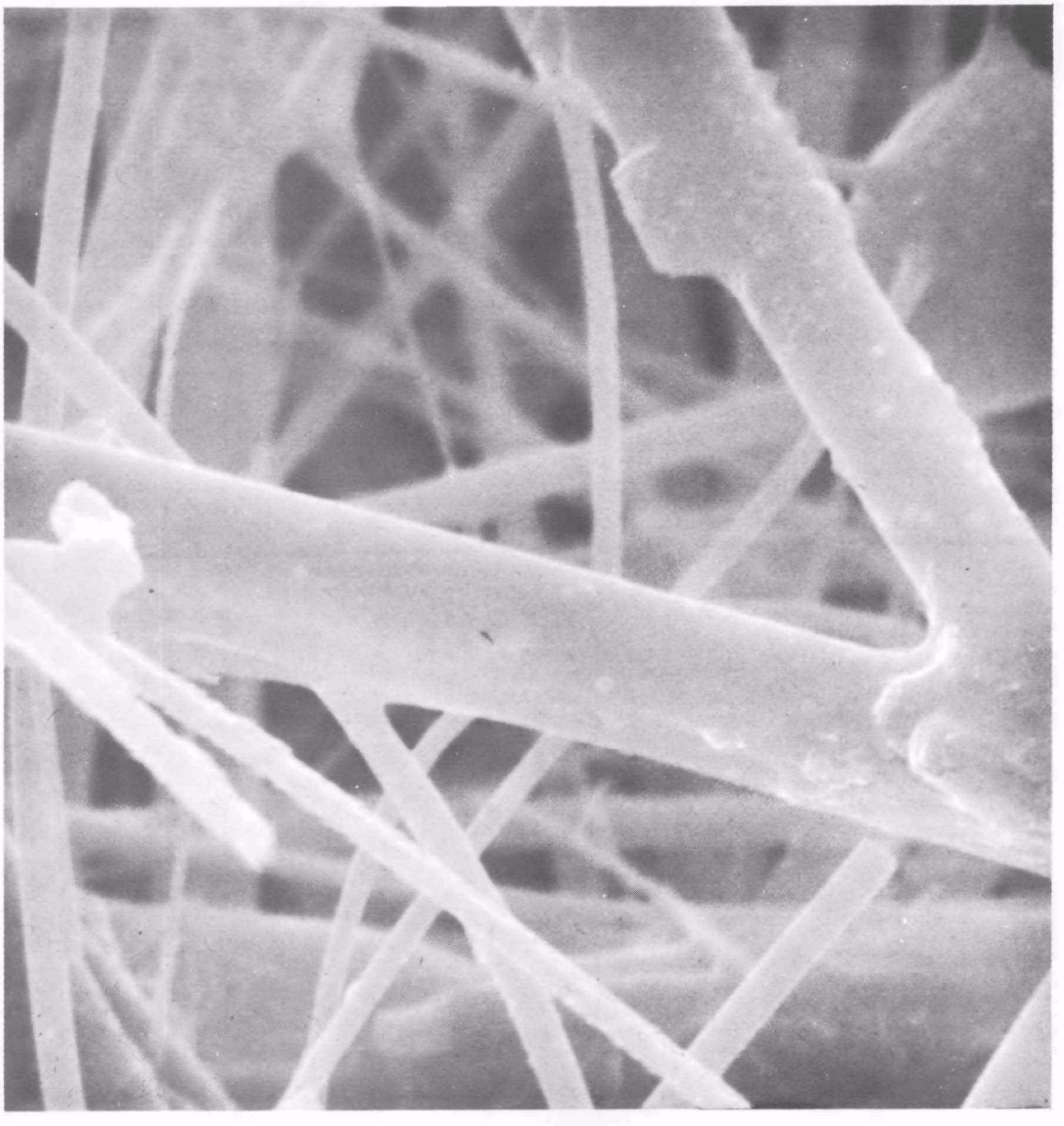

1 µm

Gelman Type A filter at 5000x magnification (scanning electron microscope photo).

Component	Concentration	
	Volume percent	(a) g/m^3
H_2O	4.0	30
CO_2	15.0	273
Fly ash before precipitator		9.16 (4 gr/ft^3)
Fly ash after precipitator		0.458 (0.2 gr/ft^3)
NO	0.050	0.63
SO_2	0.20	5.3
SO_3	0.0030 (30 ppm)	0.10
Hydrocarbons	(0.0010)	<0.1

(a) At 21°C (70°F), 1 atmosphere.

Table 1. Typical exhaust-gas composition from coal-fired boiler. (From Hillenbrand, Engdahl, and Barrett[21])

Location	Filter	H_2SO_4 ppm	H_2SO_4 gr/SCF	Total gr/SCF	H_2SO_4, % of total
Plant A	Thimble[1]	8.1	0.0147	0.0694	21
		8.1	0.0147	0.0344	43
		10.8	0.0196	0.107	18
		9.5	0.0172	0.0366	47
		9.9	0.0180	0.0645	28
		9.5	0.0172	0.0329	52
		9.5	0.0172	0.0688	25
		9.5	0.0172	0.0405	42
Plant A	Hi-volume[1]	6.9	0.0125	0.0548	23
		6.0	0.0109	0.0540	20
		8.8	0.0147	0.0255	62
		8.1	0.0050	0.0292	50
Plant A	EPA/APCO[1]	14.9	0.027	0.151	18
		13.8	0.025	0.0321	78
		7.5	0.0135	0.0308	44
		11.6	0.021	0.0388	54
		6.1	0.011	0.0242	45
		9.5	0.0172	0.0403	43
		9.5	0.0172	0.0643	27
		8.8	0.0159	0.0659	24
		8.8	0.016	0.033	48
Plant A	EPA/APCO[1]	11.0	0.020	0.033	61
		9.9	0.018	0.077	23
		9.9	0.018	0.0757	24
Plant B	EPA/APCO[2]	5.0	0.0092	0.022	42
		5.0	0.0092	0.023	40
		6.7	0.0123	0.036	34
		5.7	0.0104	0.030	35
		5.9	0.0104	0.031	34
		5.4	0.0098	0.033	30
Plant C	Hi-volume[1]	4.7	0.0085	0.0111	77
		2.8	0.0050	0.0076	66
Plant C	EPA/APCO[2]	3.5	0.0064	0.0212	30
		4.2	0.0076	0.0200	38

[1]$BaCl_2$ precipitation.
[2]NaOH titration.

Table 2. Amount of H_2SO_4 found in particulate matter by various stock sampling methods. (From Jaworowski[20]).

Solute Conc. (Wt.%)	NMD(μm)	MMD(μm)	σ_g
1.00% Uranine	0.050	0.140	1.80
0.1% Uranine	0.028	0.089	1.86
0.01% Uranine	0.017	0.050	1.82
1.0% NaCl	0.023	0.061	1.77

Table 3. Size distribution of aerosols produced in Collison atomizer with impactor (water solvent).

Solute Conc. (Wt.%)	NMD(μm)	MMD(μm)	σ_g
1.0% Uranine	0.054	0.103	1.41
0.1% Uranine	0.028	0.049	1.49
0.01% Uranine	0.016	0.028	1.45

Table 4. Liu's data on performance of Collison atomizer with impactor (water solvent). (From Liu[48])

Aerosol Description	Generation Method	NMD(μm)	MMD(μm)	σ_g
0.002% Uranine by wt. in ethanol	Spinning Disk	0.75	0.79	1.14
0.005% Uranine by wt. in ethanol	Spinning Disk	1.06	1.10	1.12
0.02% Uranine by wt. in ethanol	Spinning Disk	1.43	1.49	1.12
0.1% Uranine by wt. in ethanol	Spinning Disk	2.68	2.84	1.15
1.0% Uranine by wt. in ethanol	Spinning Disk	5.82	5.98	1.10
Paper Mulberry Pollen	Mechanical Dispersion	12.9	13.1	1.07
Ragweed Pollen	Mechanical Dispersion	26.2	26.7	1.08
Fly Ash	Mechanical Dispersion	1.10	5.61	2.09

Table 5. Size distributions of experimental aerosols.

Aerosol	mmd(μm)	Velocity(cm/sec)	Temp(°C)	% Pen. @ 7.0 μg/cm^2 loading	Filter Type
Uranine	0.09	51	21	0.10	Microquartz (Q)
			120	0.05	Q
			260	0.03	Q
			21	0.14	Type A (A)
			120	0.05	A
		51	260	0.02	A
		18	21	<0.01	Q
			120	<0.01	Q
		18	260	<0.01	Q
		6	21	<0.01	Q
			120	<0.01	Q
		6	260	<0.01	Q
		0.5	21	<0.01	Q
			120	<0.01	Q
Uranine	0.09	0.5	260	<0.01	Q
Uranine	0.14	51	21	0.10	Q
		51	260	0.01	Q
		18	21	0.03	Q
		18	260	<0.01	Q
		6	21	<0.01	Q
		6	260	<0.01	Q
		0.5	21	<0.01	Q
Uranine	0.14	0.5	260	<0.01	Q
NaCl	0.06	51	21	0.02	Q
NaCl	0.06		260	<0.01	Q
NaCl	0.06		537	<0.01	Q
Uranine	0.79,1.10, 1.49,2.84, 5.98	51	21	<0.01	Q
				<0.01	Q

Table 6. Effect of temperature on filtration efficiency.

	120°C(1)	205°C(1)
	% of Total H_2SO_4 Catch (2)	% of Total H_2SO_4 Catch (2)
S.S. Coil at Test Temperature	61	8
Filter at Test Temperature	32	11
Two Impingers + Backup Filter	7	81
	100 Total	100 Total

(1) H_2SO_4 Dewpoint ≈170°C
(2) Average of two trials

Table 7. H_2SO_4 distribution in sampling train.

Vel(cm/sec)	T(°C)	Theoretical - % Penetration D=0.4(1) d=0.14(2) σ_g=1.0	D=0.5 d=0.14 σ_g=1.0	D=0.6 d=0.14 σ_g=1.0	D=0.4 d=0.14 σ_g=1.8(3)	Experimental-% Penetration d=0.14 σ_g=1.80
5.1	21	<0.01	0.10	0.16	0.01	0.01
18.3	21	<0.01	0.10	0.13	0.02	0.03
51.0	21	<0.01	<0.01	0.04	0.01	0.10
5.1	260	<0.01	0.01	0.13	<0.01	<0.01
18.3	260	<0.01	0.01	0.11	0.01	<0.01
51.0	260	<0.01	<0.01	0.03	0.01	0.01

(1) D = Fiber diameter in μm.
(2) d = Aerosol mass median diameter in μm.
(3) Aerosol size distribution divided into 10 equal mass divisions based on an aerosol σ_g=1.8.

Table 8. Theoretical and experimental penetrations of "Microquartz" filter media.

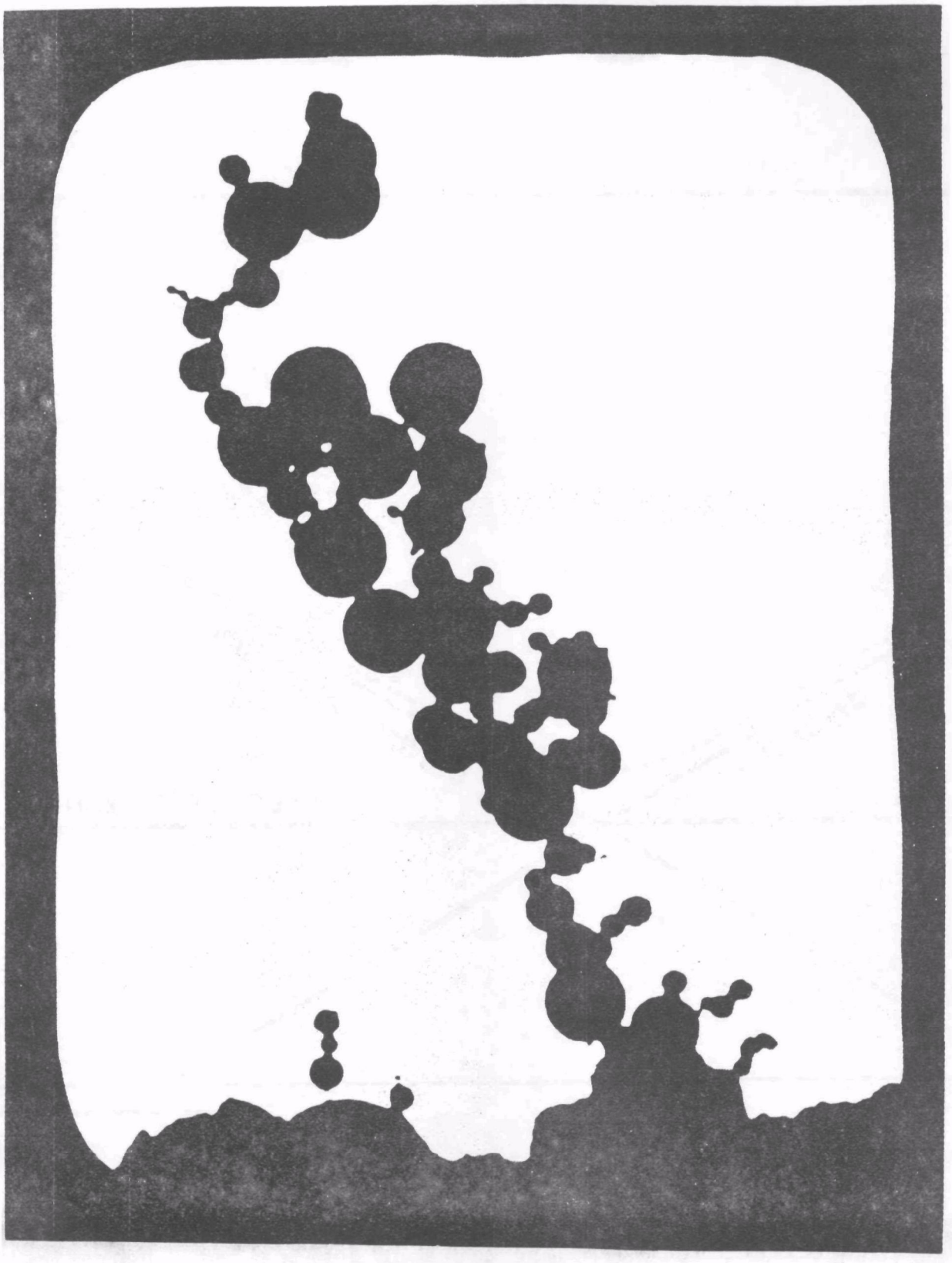

Figure 1. Structure of "tree" on a metal fiber. (From Davies [12]).

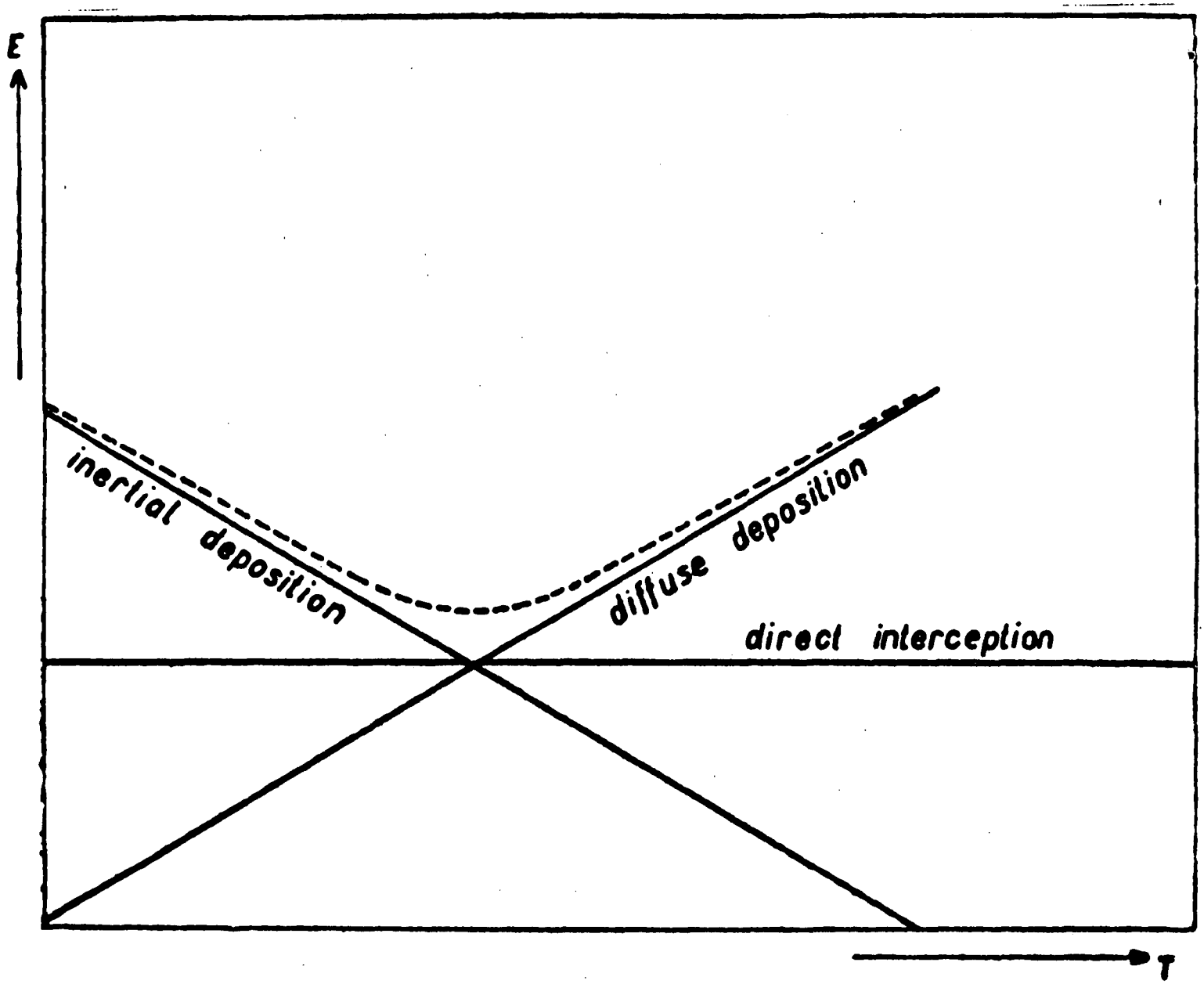

Figure 2. Effect of temperature on penetration (theoretical) (From Pich[13]).

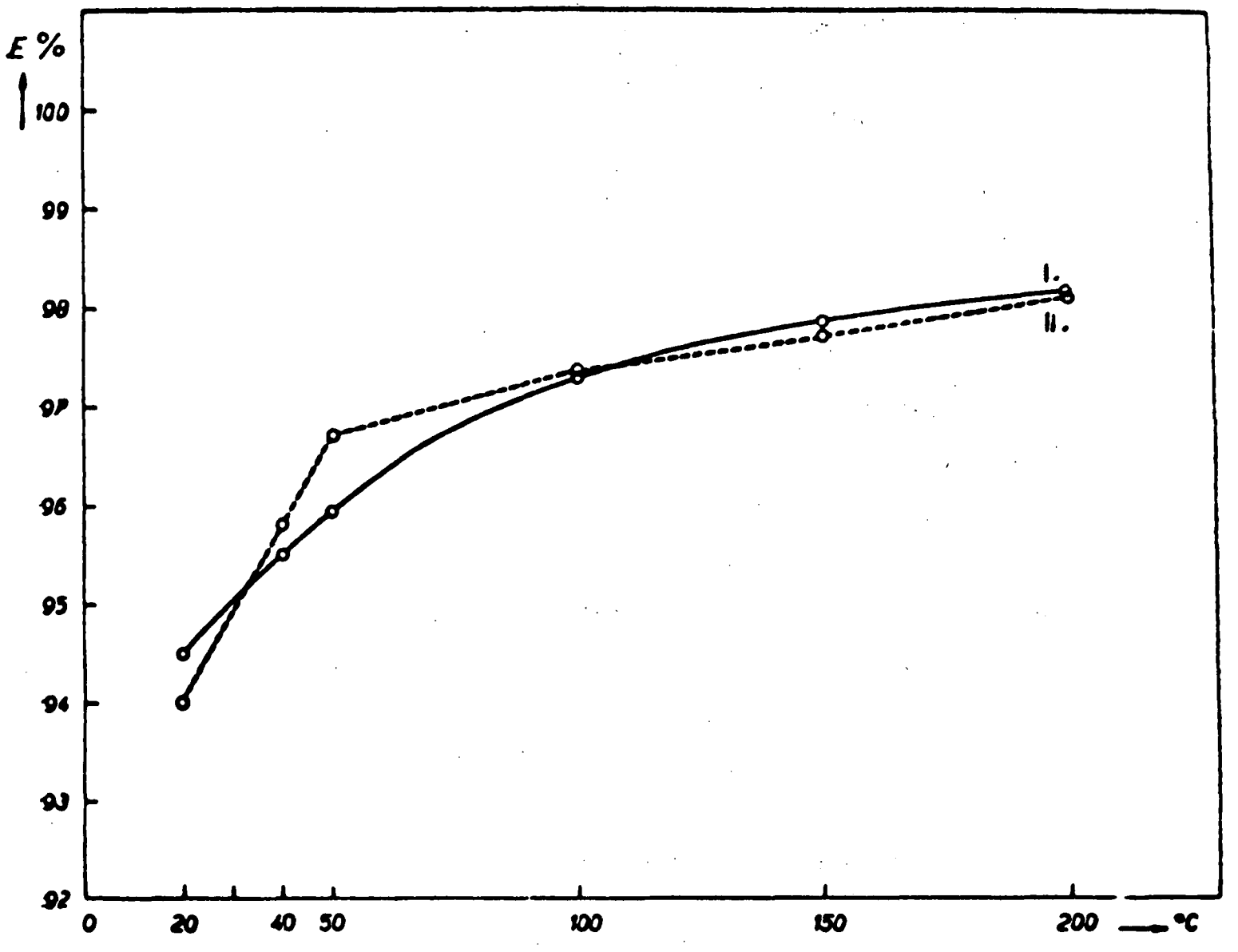

Figure 3. Effect of temperature on penetration (experimental) (From Pich[13]).

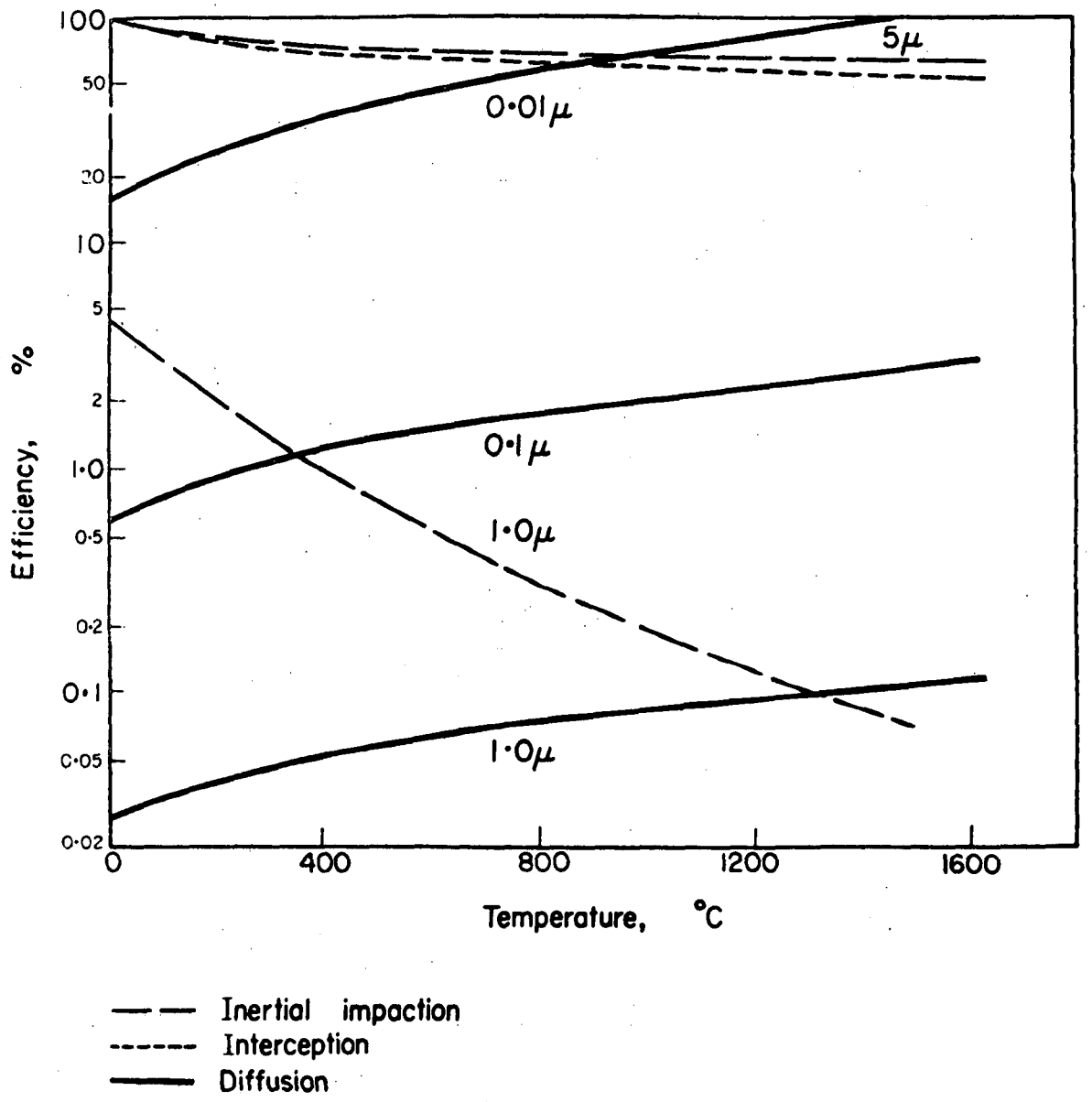

Figure 4. Effect of temperature on collection mechanisms of impaction, interception and diffusion. (From Thring and Strauss [17]).

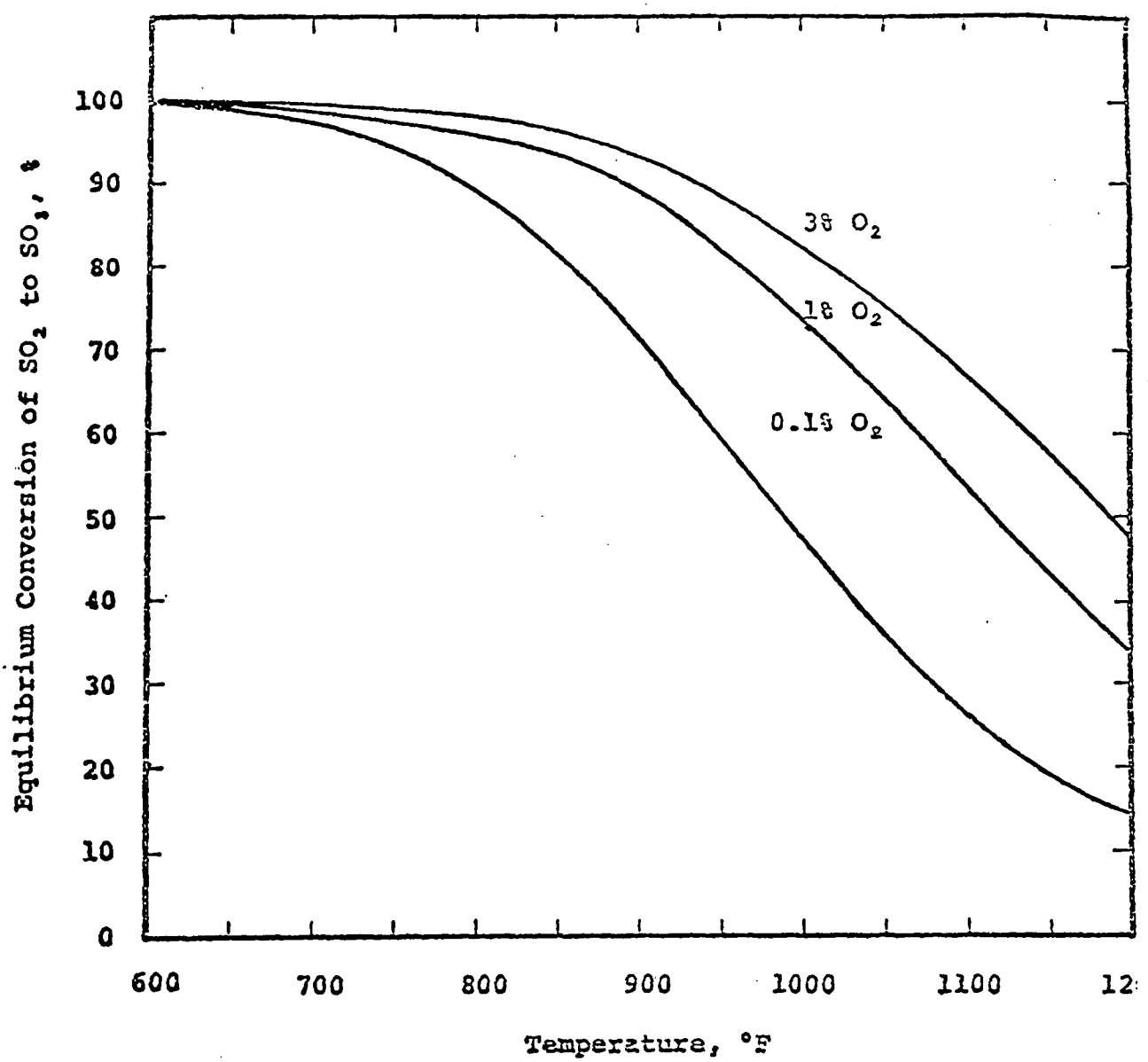

Figure 5. Equilibrium conversion of SO_2 to SO_3. (From Hillenbrand, Engdahl, and Barrett[21])

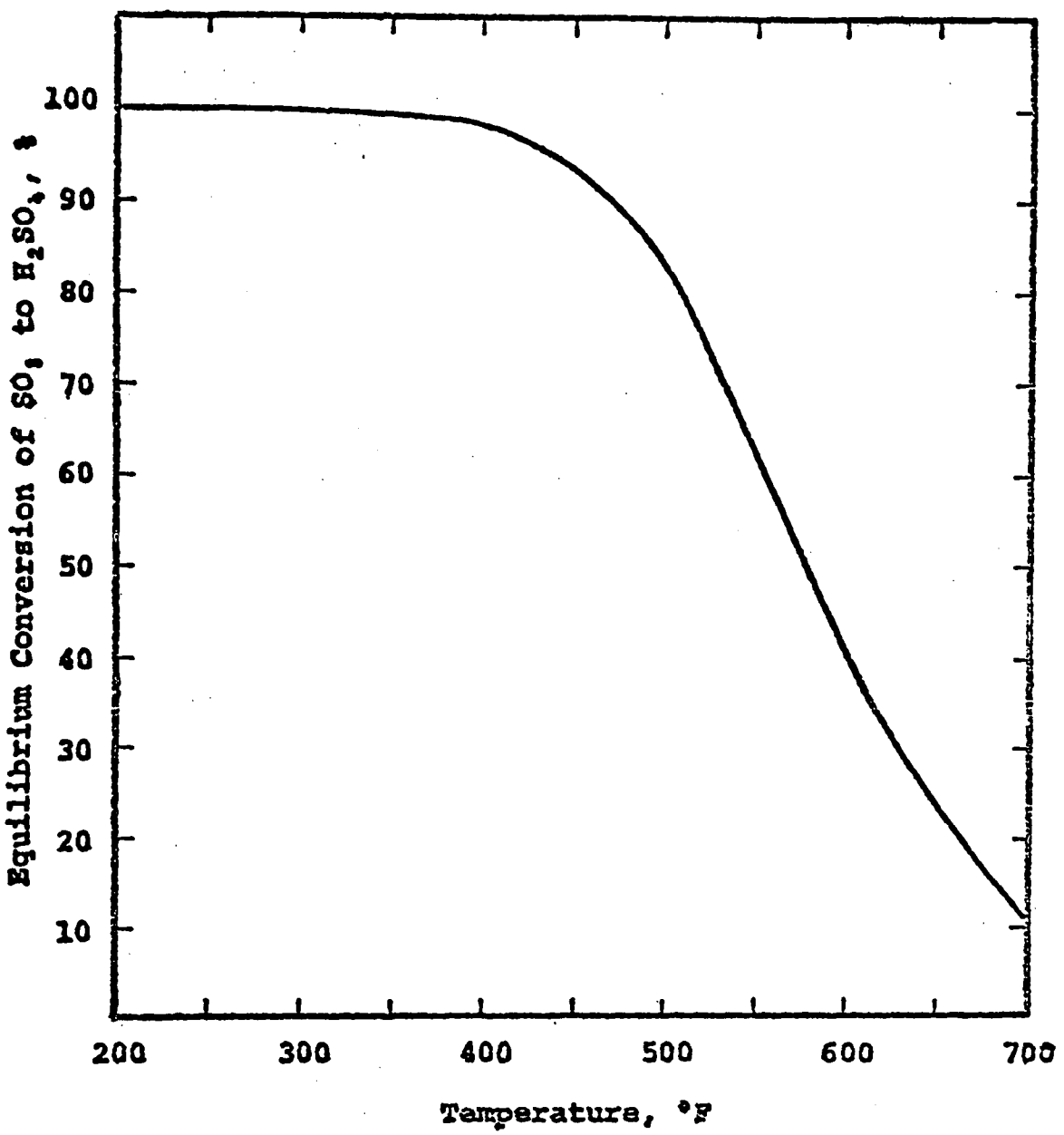

Figure 6. Equilibrium conversion of SO_3 to H_2SO_4 at 8.0 vol% H_2O in flue gas. (From Hillenbrand, Engdahl, and Barrett [21])

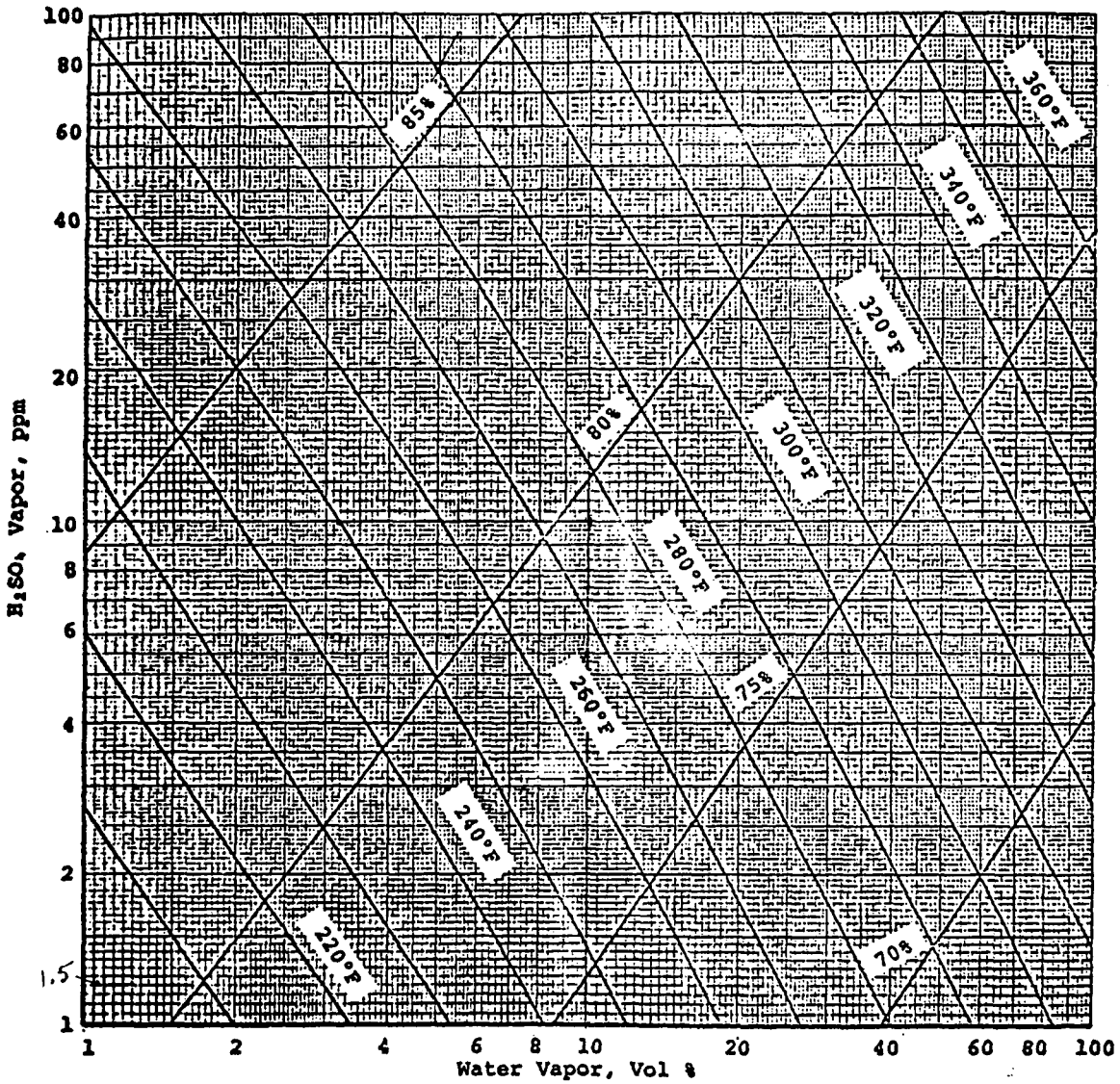

Figure 7. Dewpoint and condensate composition for vapor mixtures of H_2O and H_2SO_4 at 760 mm Hg total pressure. (From Abel[26] and Greenewalt[27])

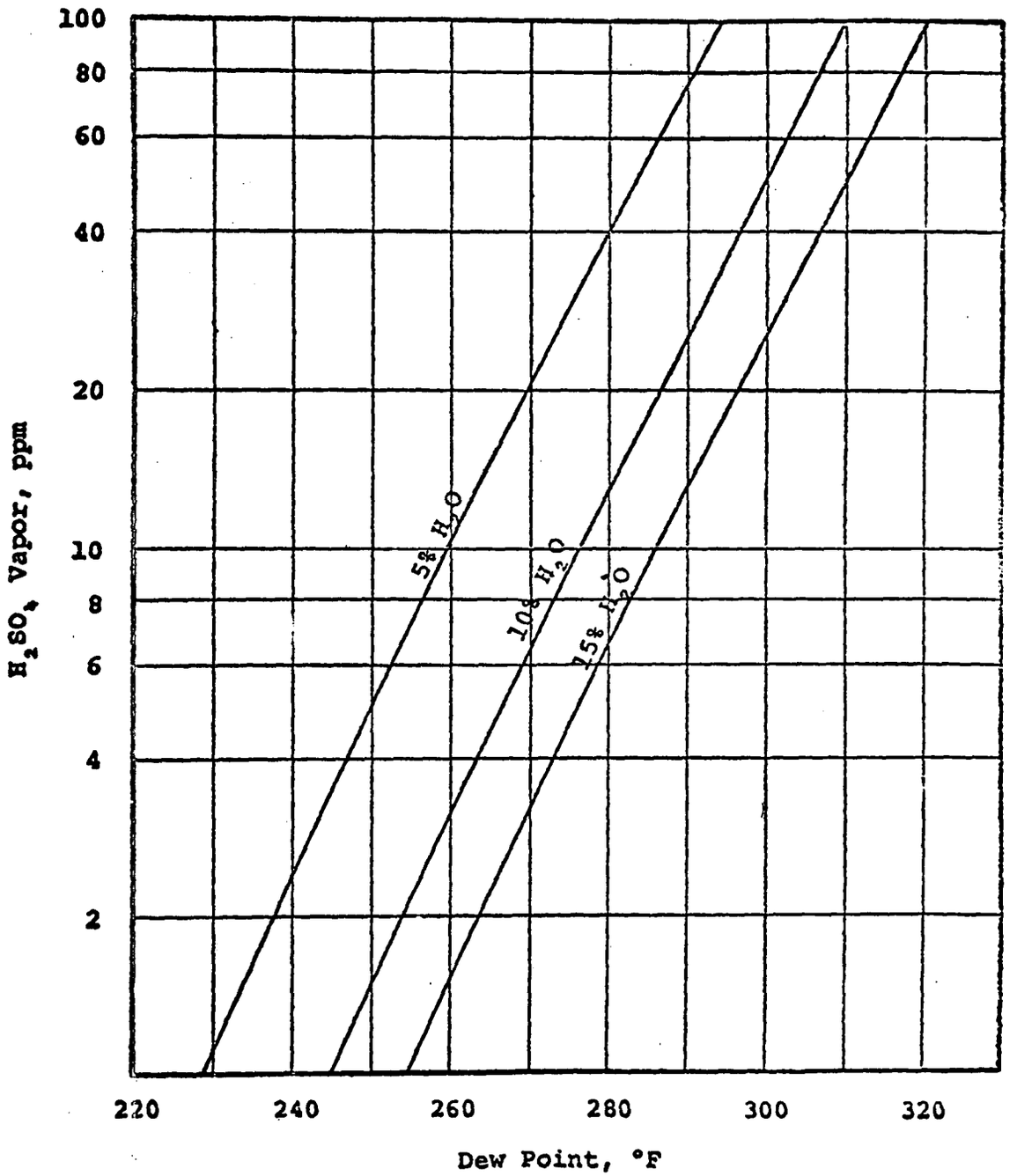

Figure 8. H_2SO_4 dewpoint for typical flue gas moisture concentrations. (From Abel[26] and Greenewalt[27])

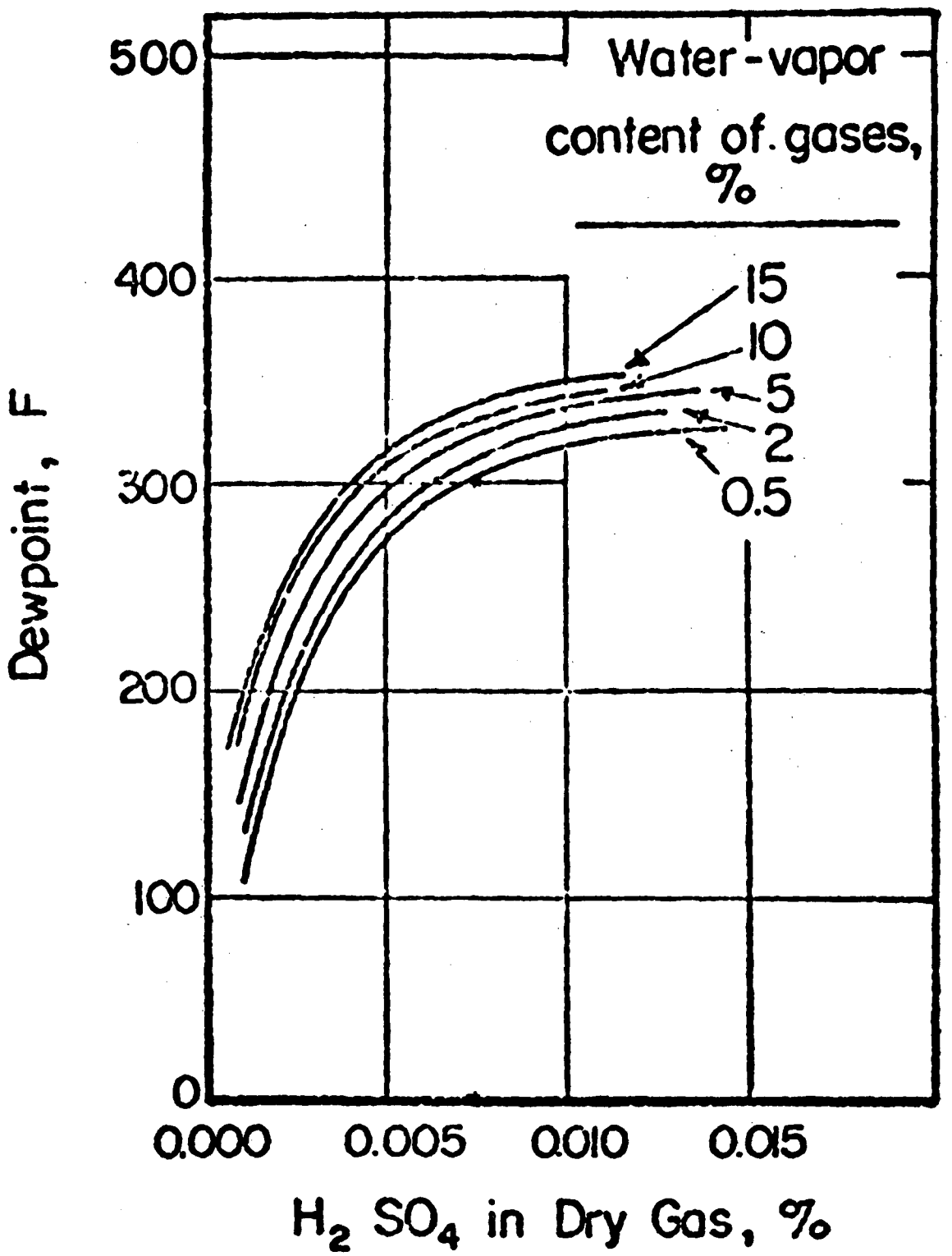

Figure 9. Variation of dewpoint with H_2SO_4 content for gases having different H_2O contents. (From Matty, and Diehl [28])

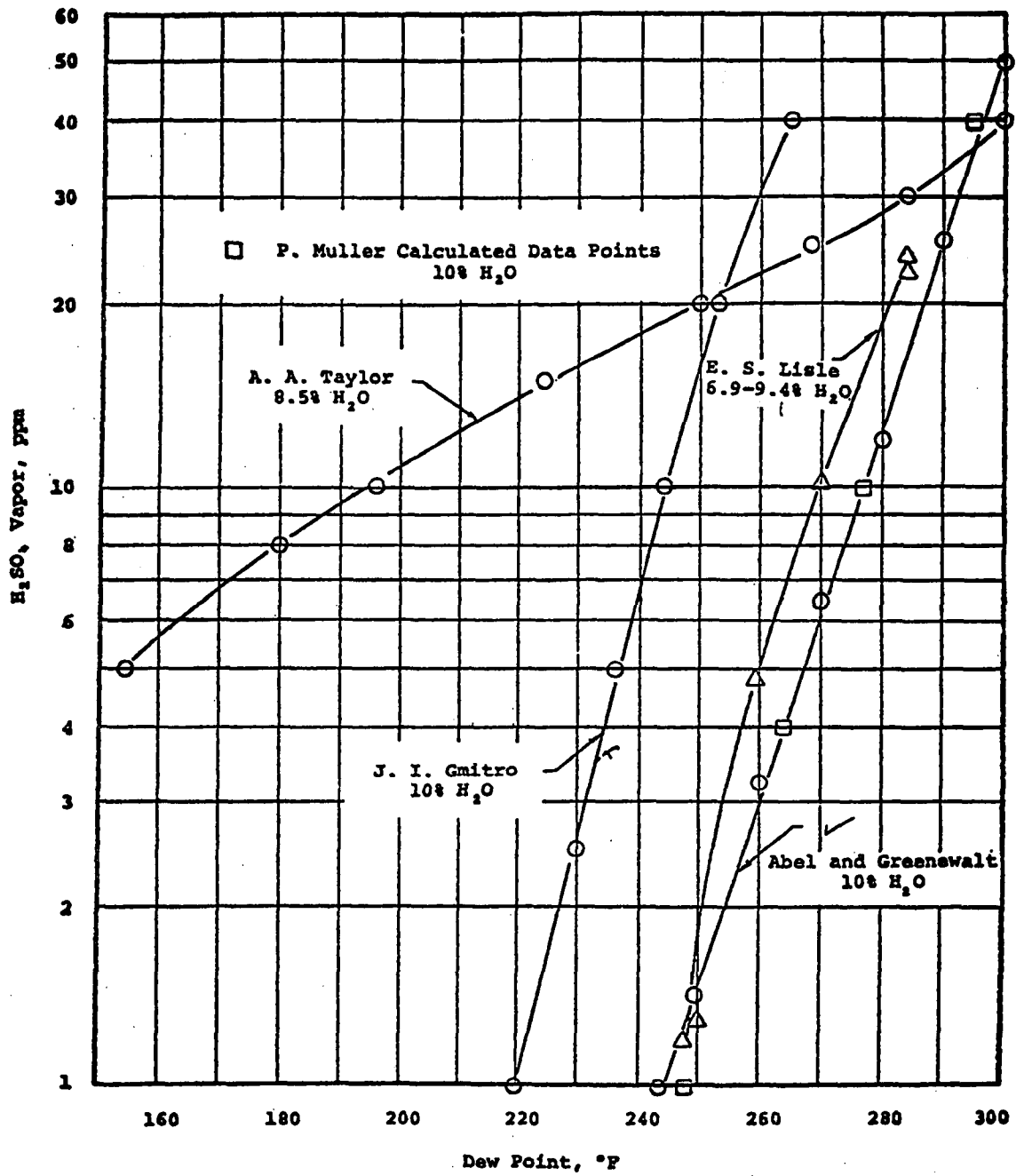

Figure 10. H_2SO_4 dewpoint obtained by various investigators. Abel and Greenewalt [2,4,26,27], Gmitro [31], Lisle [30], Muller [25], and Taylor [29].

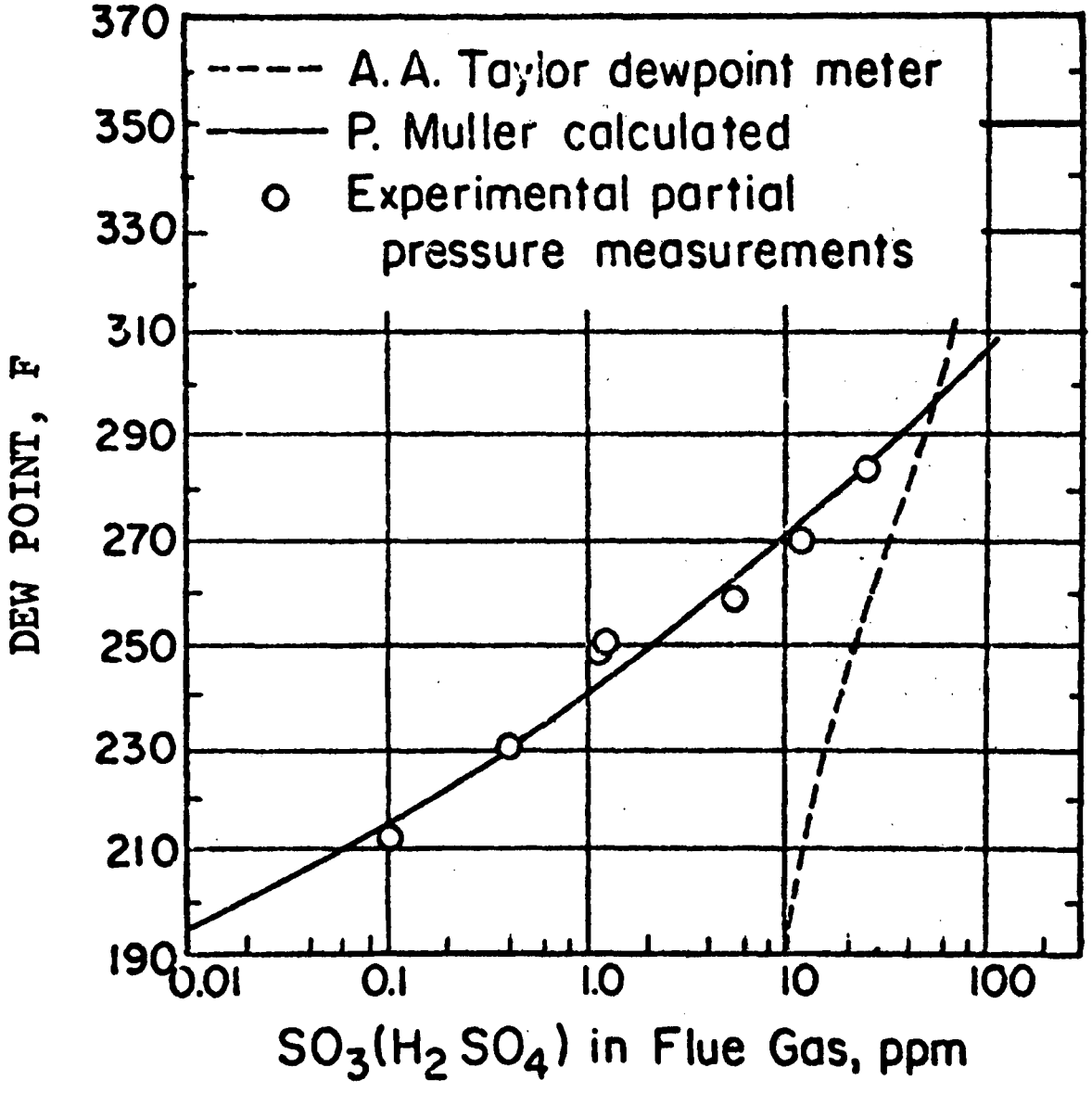

Figure 11. Dewpoint as a function of H_2SO_4 concentration (From Taylor[29] and Mueller[25])

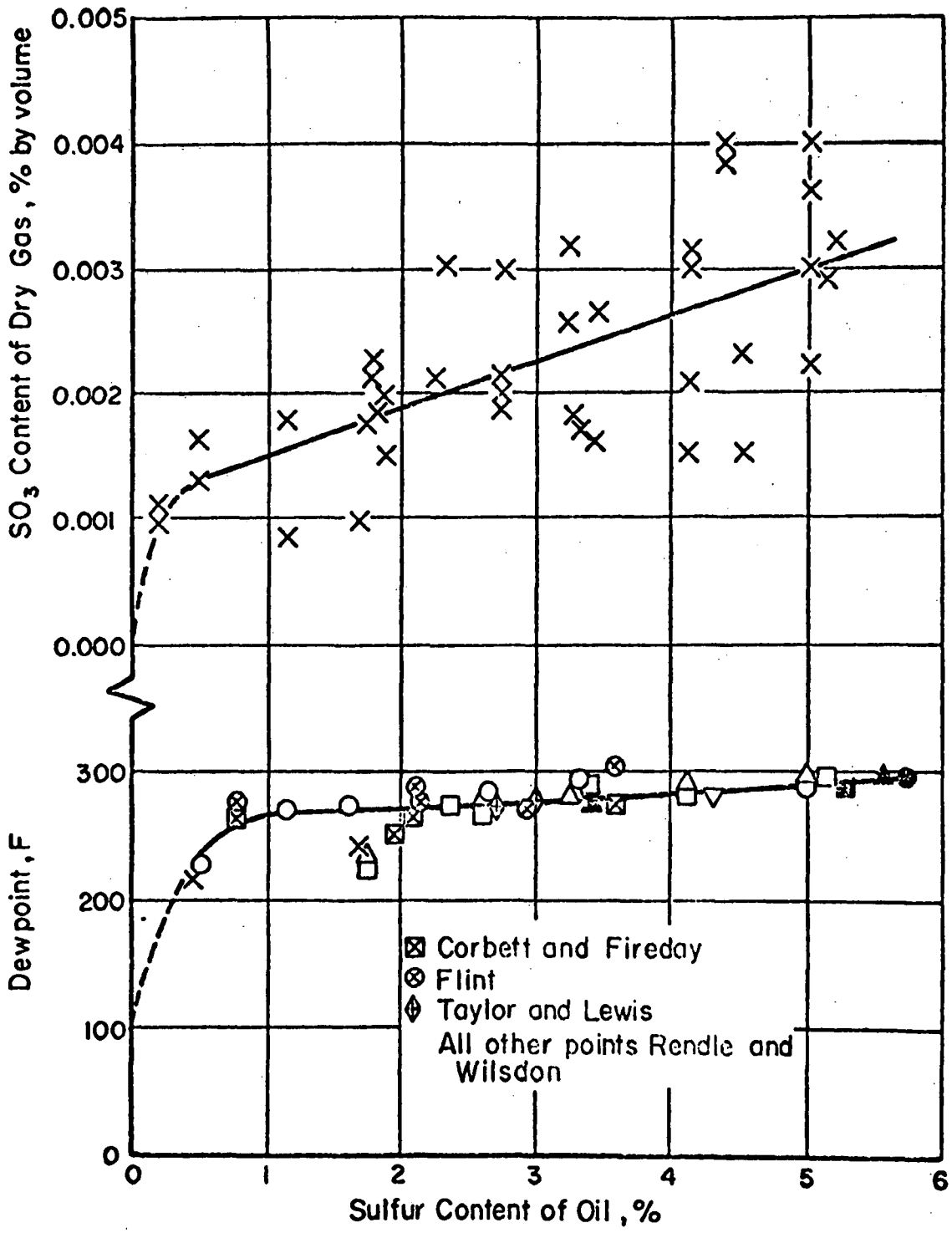

Figure 12. Relation of dewpoint and SO_3 content of combustion gases to sulfur content of oil. (From Corbett and Fireday[35], Flint et al.[34], Taylor and Lewis[33], and Rendle and Wilson[32])

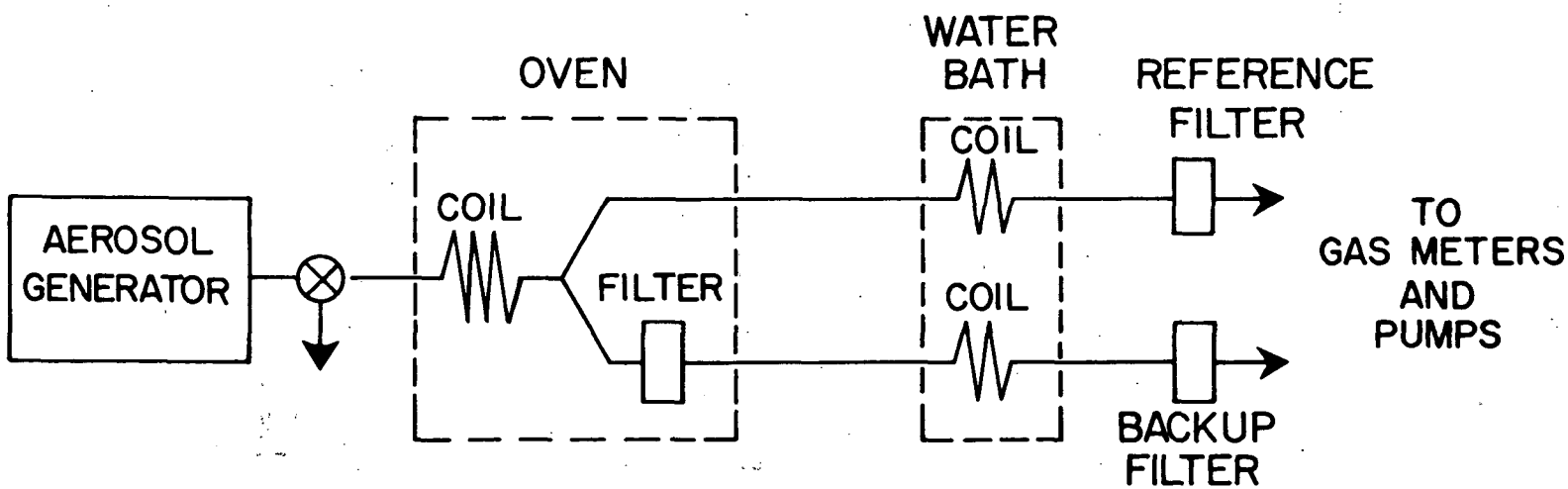

Figure 13. General arrangement of test apparatus.

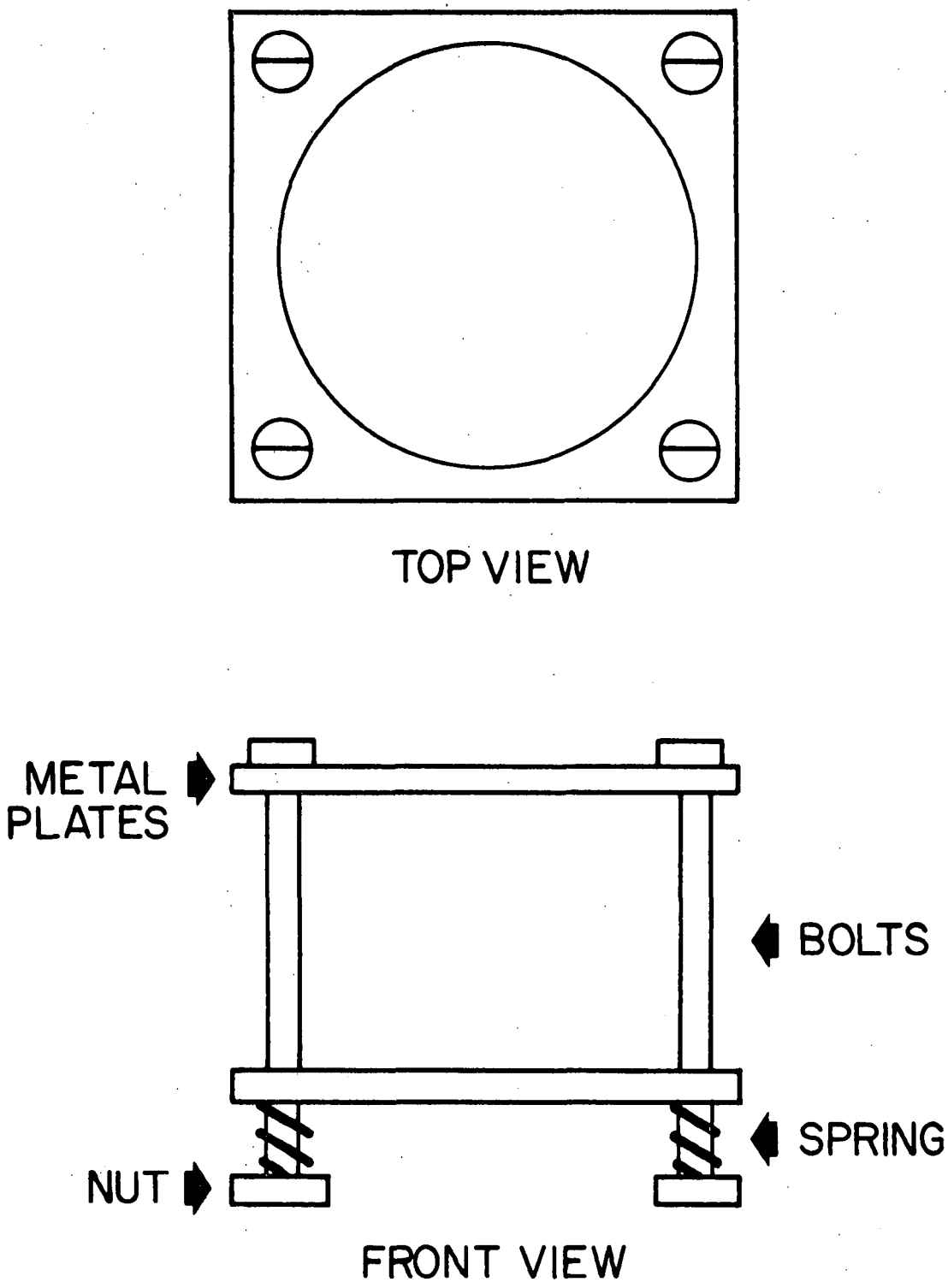

Figure 14. Clamp assembly for glass filter holder.

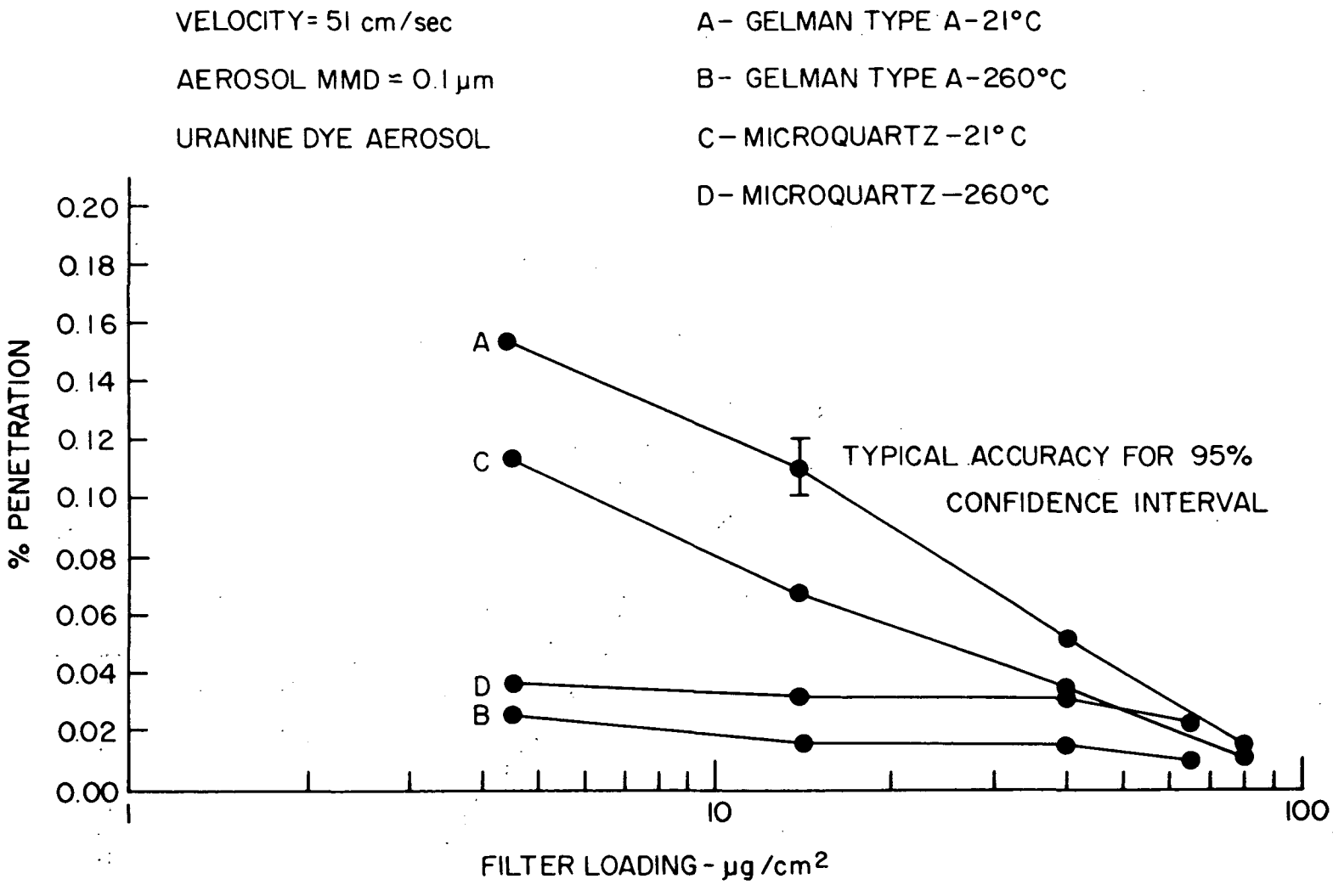

Figure 15. Effect of filter loading on penetration.

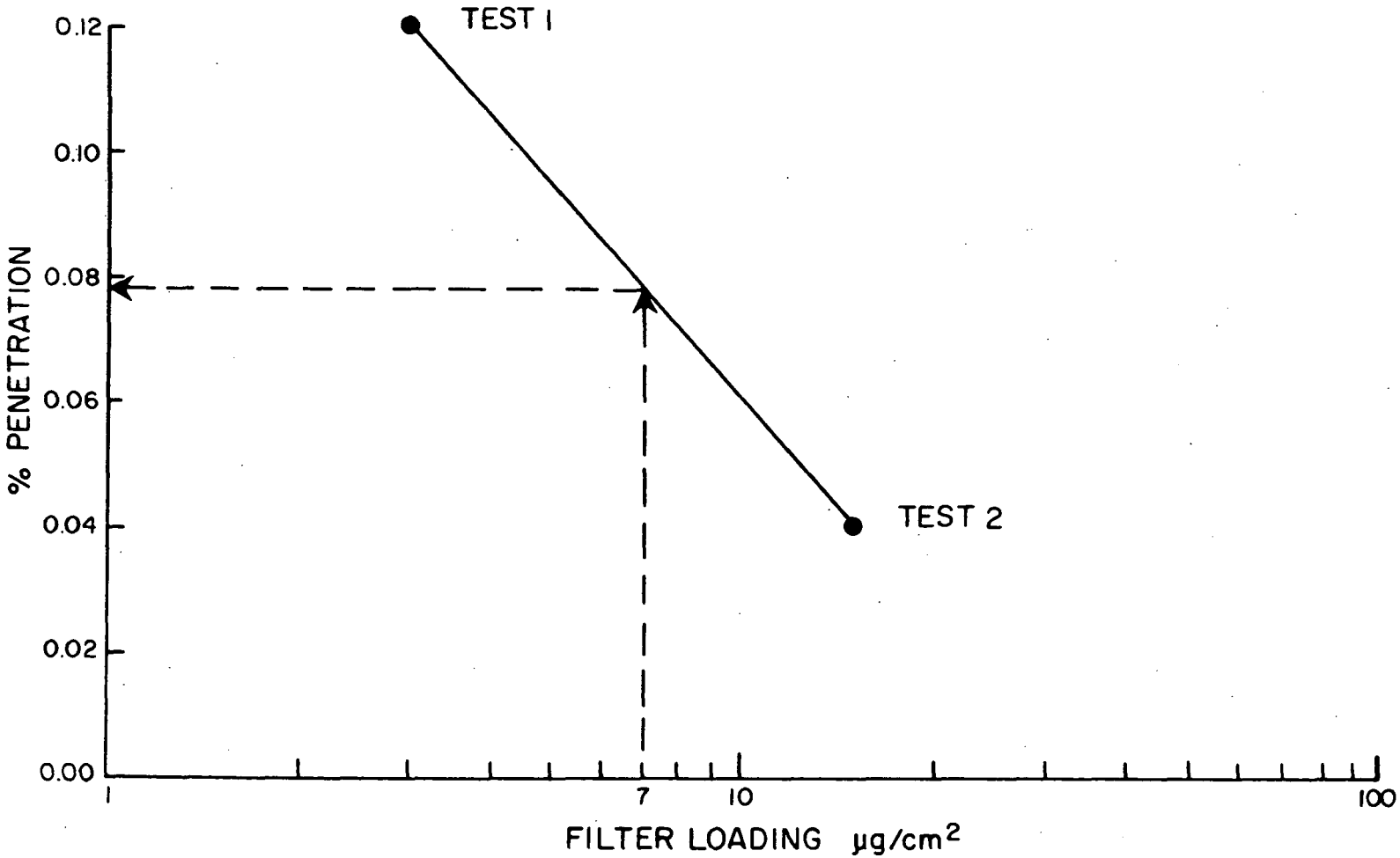

Figure 16. Method to determine penetration at 7.0 µg/cm^2 loading.

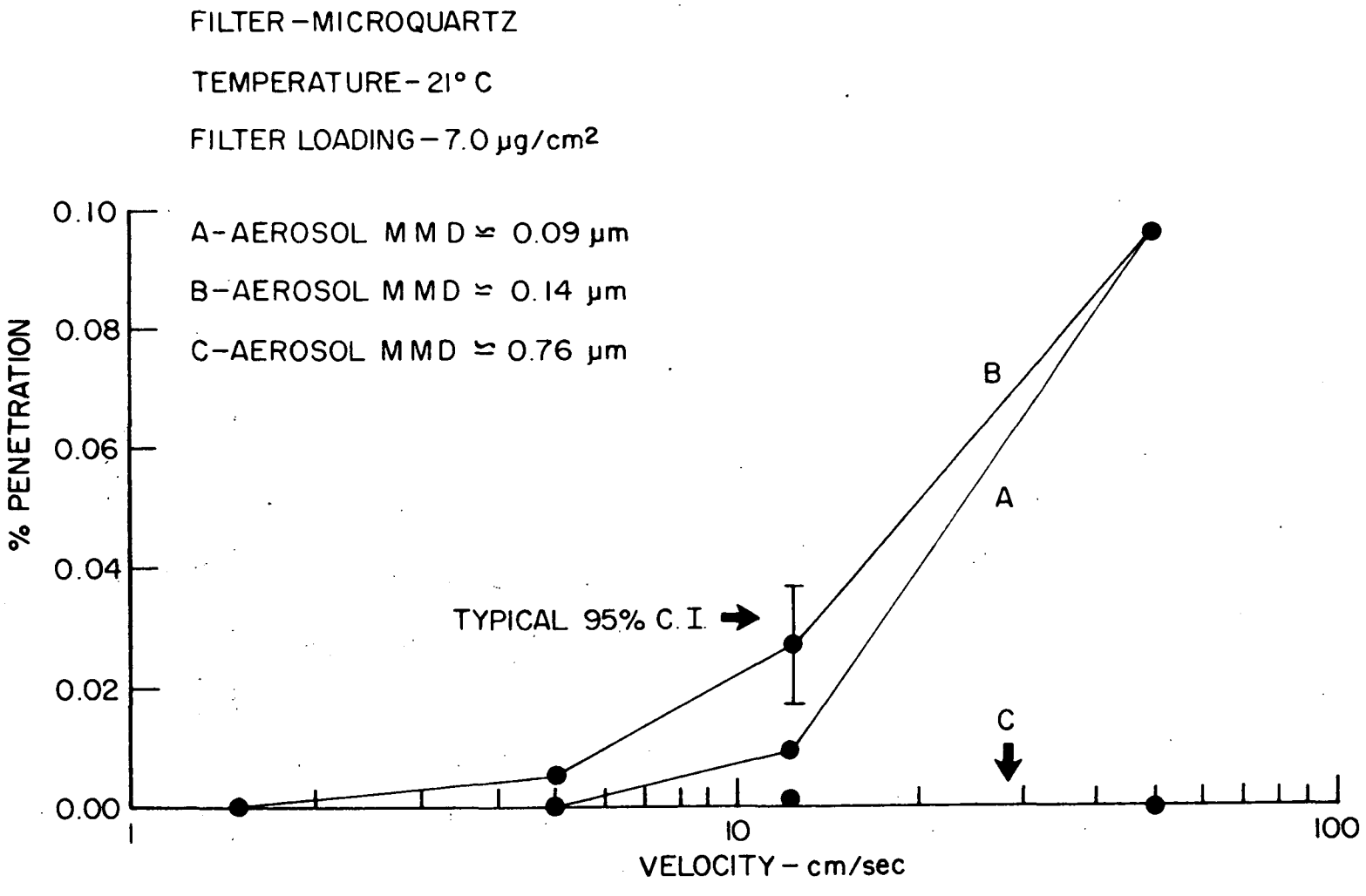

Figure 17. Effect of velocity on penetration("Microquartz"Filter).

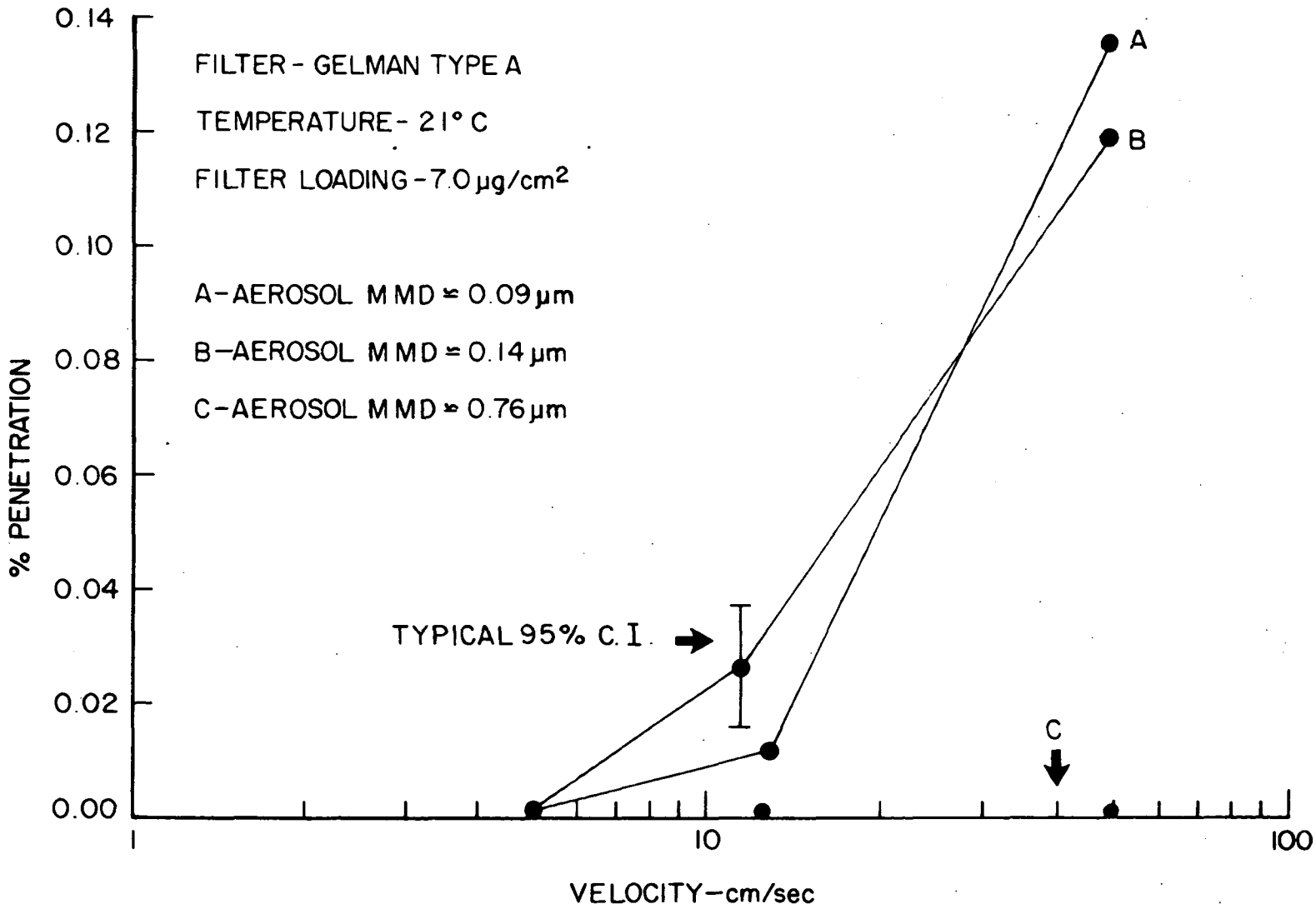

Figure 18. Effect of velocity on penetration (Gelman Type A Filter)

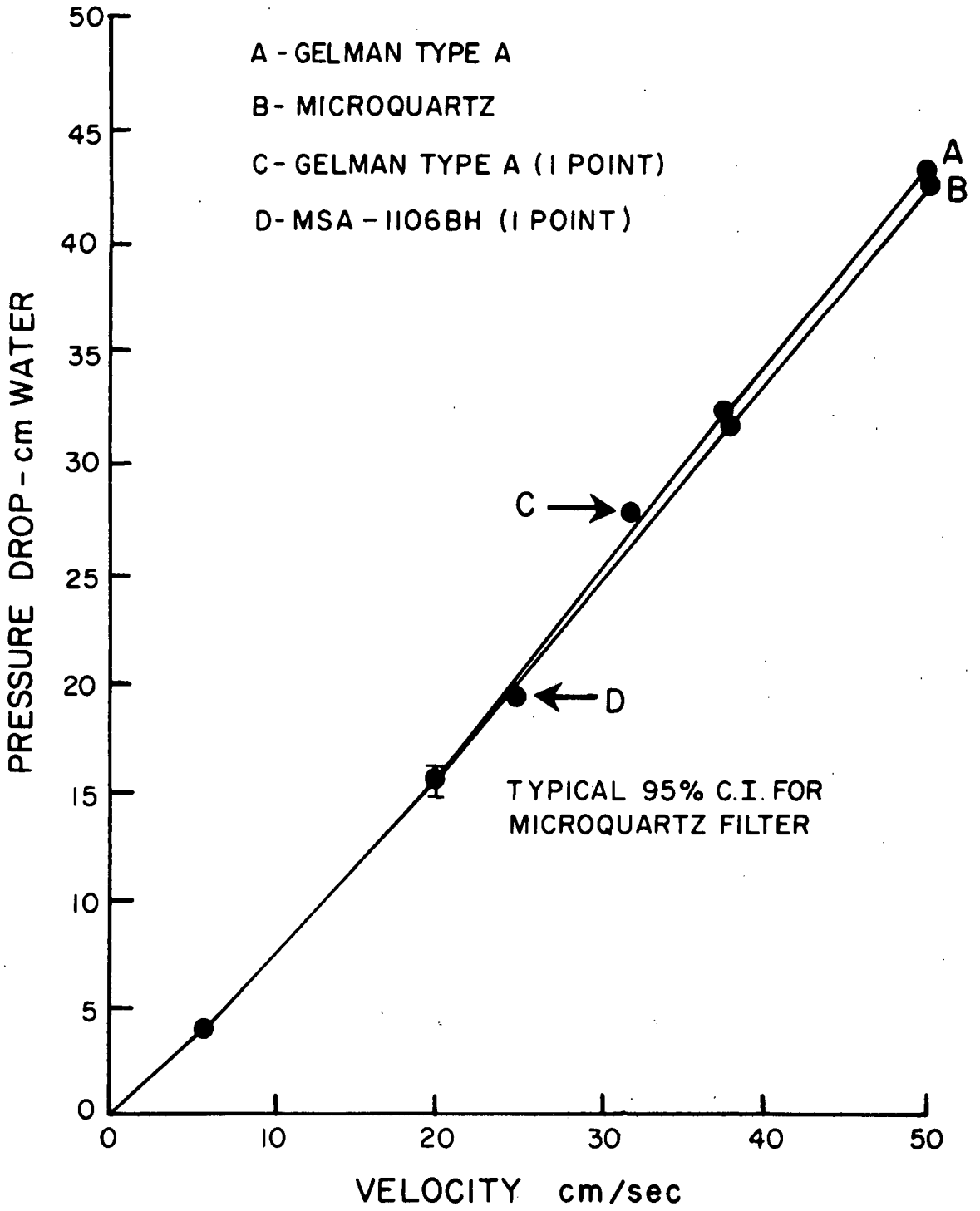

Figure 19. Pressure drop vs. velocity.

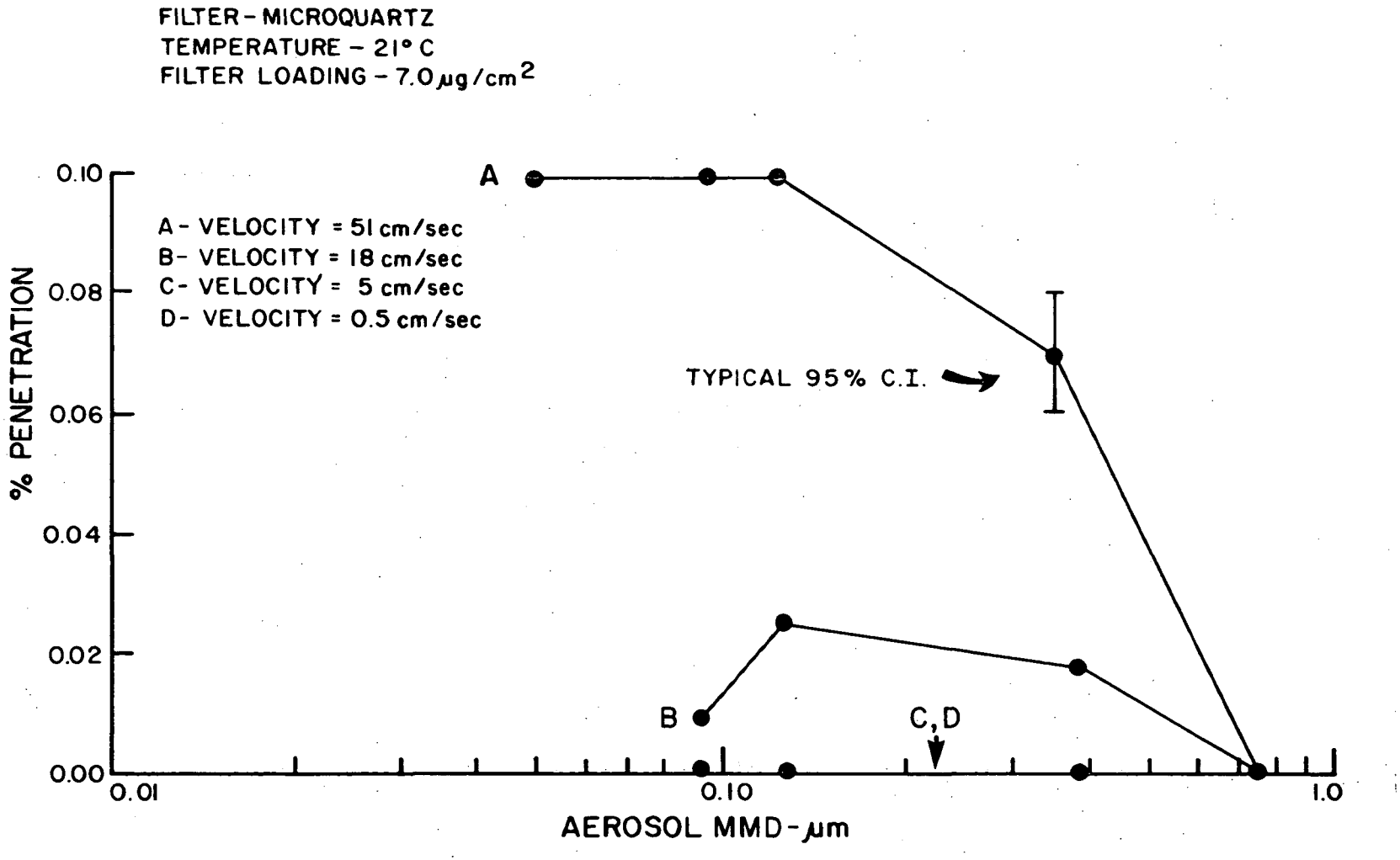

Figure 20. Effect of particle size on penetration ("Microquartz"Filter)

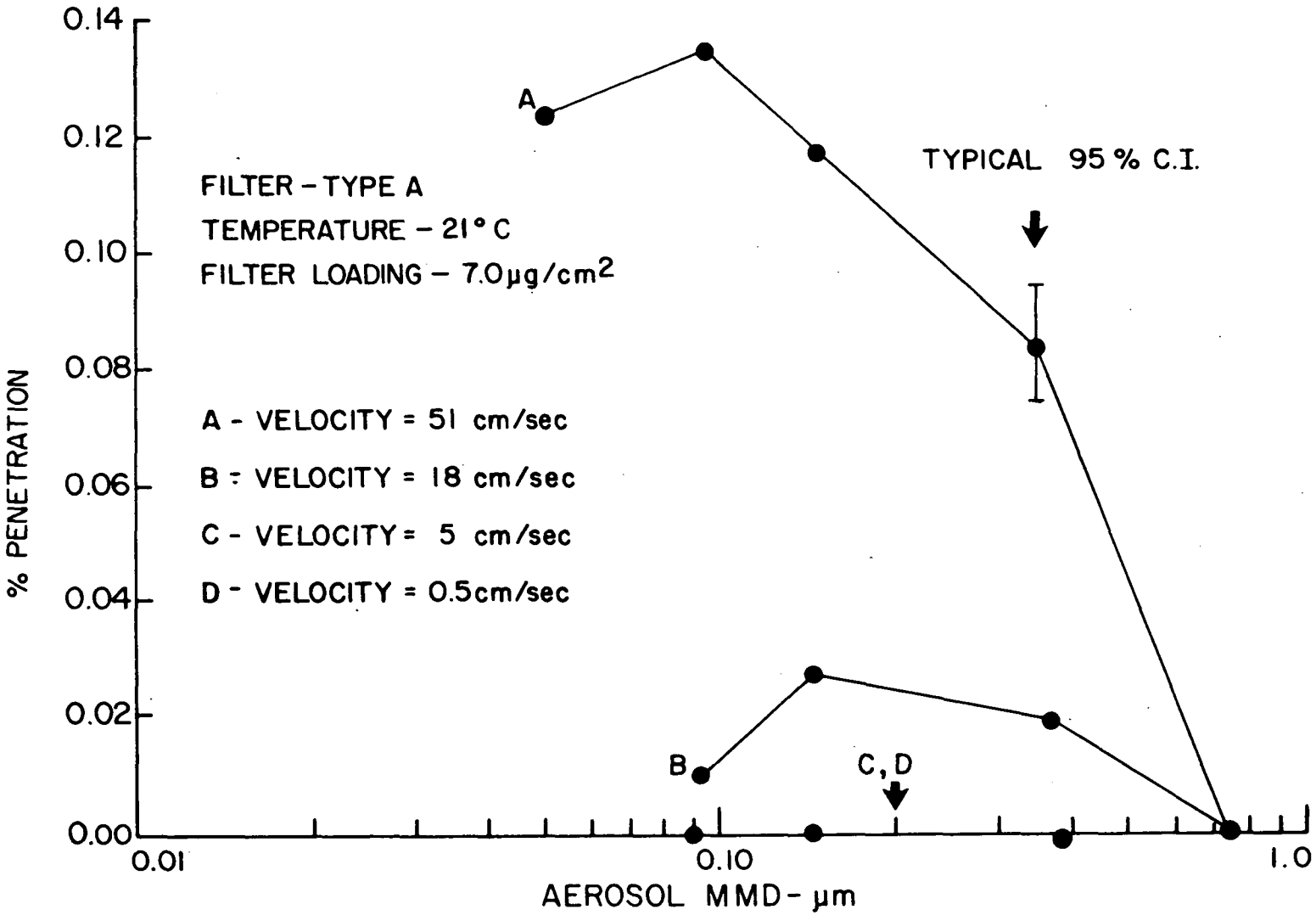

Figure 21. Effect of particle size on penetration (Gelman Type A Filter)

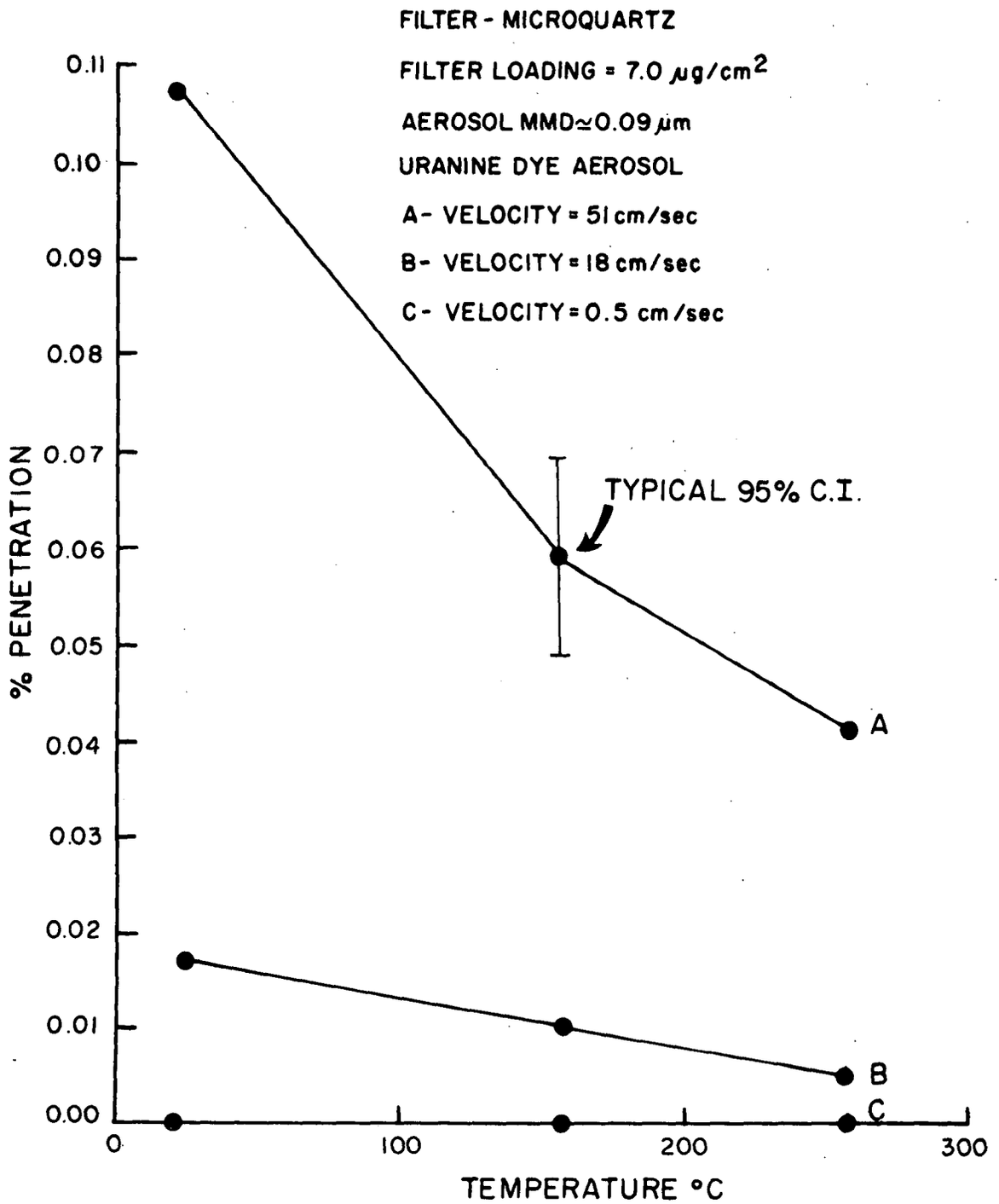

Figure 22. Effect of temperature on penetration

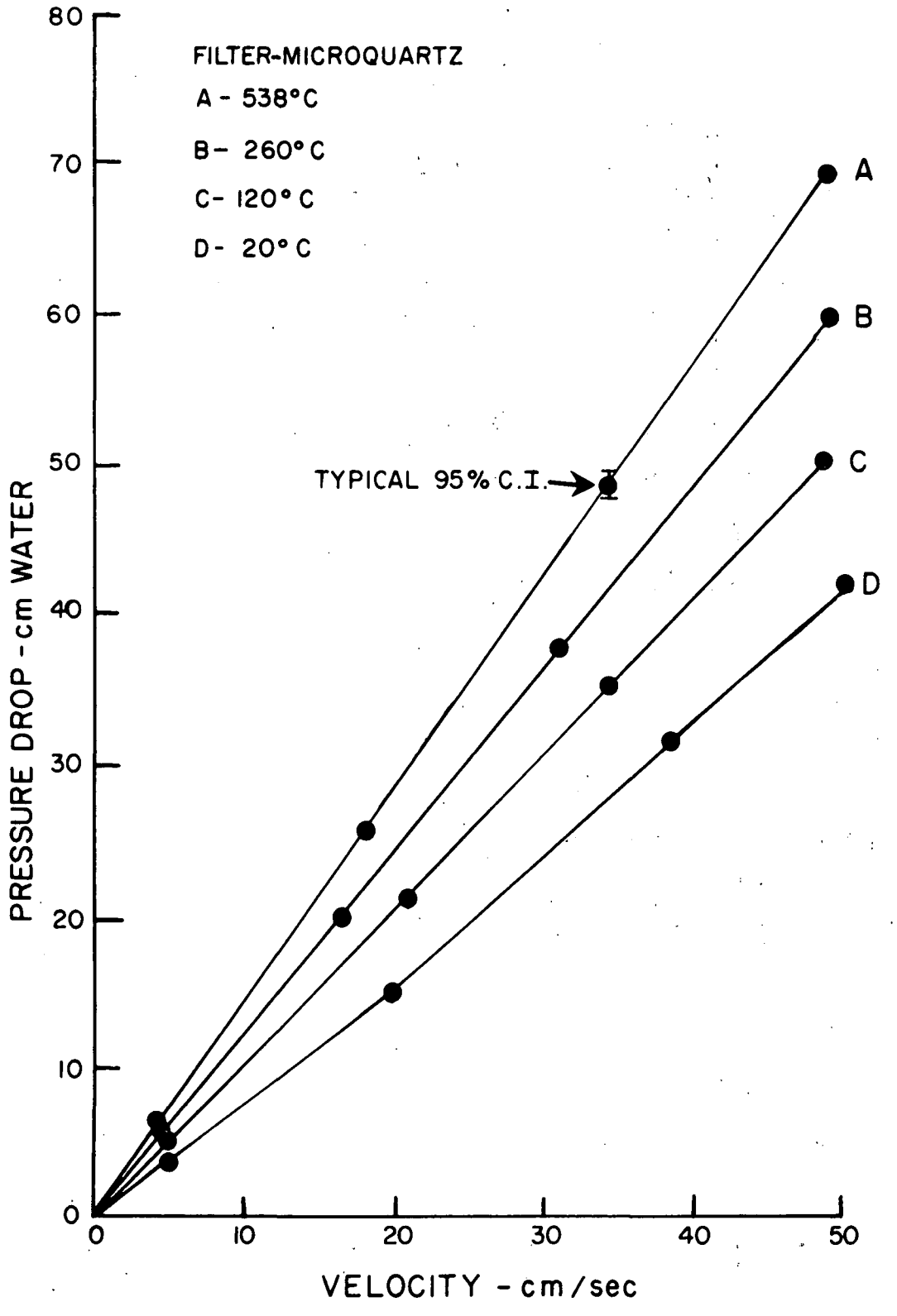

Figure 23. Pressure drop vs. velocity at elevated temperatures

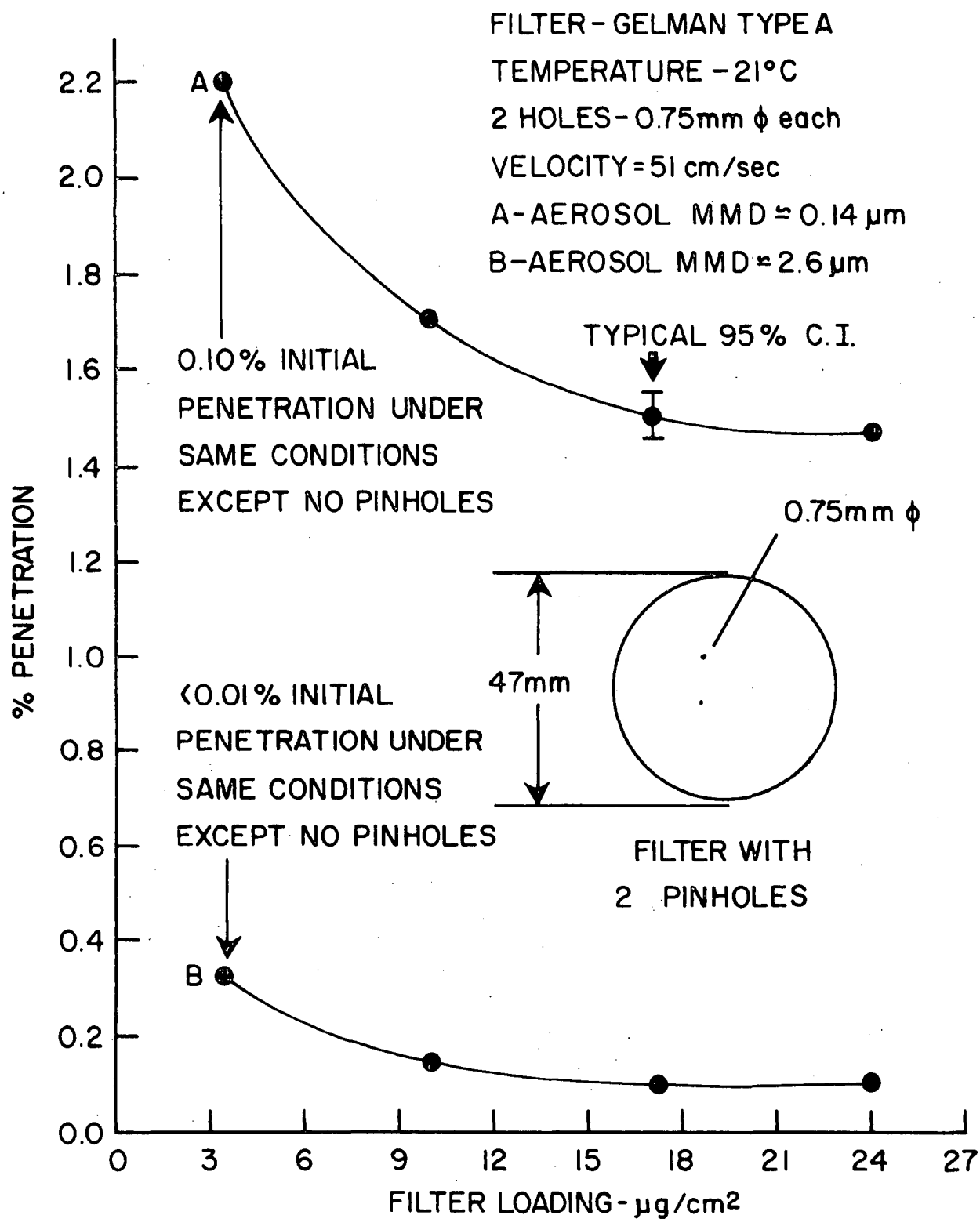

Figure 24. Effect of pinholes on penetration

TECHNICAL REPORT DATA
(Please read Instructions on the reverse before completing)

1. REPORT NO.	2.	3. RECIPIENT'S ACCESSION NO.
EPA-600/2-76-192		

4. TITLE AND SUBTITLE	5. REPORT DATE
FILTRATION CHARACTERISTICS OF GLASS FIBER FILTER MEDIA AT ELEVATED TEMPERATURES	July 1976
	6. PERFORMING ORGANIZATION CODE

7. AUTHOR(S)	8. PERFORMING ORGANIZATION REPORT NO.
Dale A. Lundgren and Thomas C. Gunderson	

9. PERFORMING ORGANIZATION NAME AND ADDRESS	10. PROGRAM ELEMENT NO.
Department of Environmental Engineering Sciences University of Florida Gainesville, Florida 32601	1AA010
	11. CONTRACT/GRANT NO.
	R803126-01

12. SPONSORING AGENCY NAME AND ADDRESS	13. TYPE OF REPORT AND PERIOD COVERED
Environmental Sciences Research Laboratory Office of Research and Development United States Environmental Protection Agency Research Triangle Park, North Carolina 27711	Final 7/74 - 7/75
	14. SPONSORING AGENCY CODE
	EPA - ORD

15. SUPPLEMENTARY NOTES

16. ABSTRACT

Particle collection characteristics of a newly developed, high-purity "Microquartz" fiber filter media and a Gelman Type A glass fiber filter media were evaluated over a range of temperatures (20°C to 540°C), particle sizes (0.05 μm to 26 μm), gas velocities (0.5 cm/sec to 51 cm/sec), and particle volatilities. Both types of high efficiency filters proved adequate (>99.9% efficiency) for sampling nonvolatile particles over the above variable ranges. Nonvolatile particle penetration decreased with increasing temperature and increasing filter loading.

The effect elevated temperature had on particle collection characteristics was not a determining factor in the application of high efficiency filters. The main problems encountered in the high temperature environment were filter holder leakage and volatilization of gas-borne particles that passed through the filter media.

17. KEY WORDS AND DOCUMENT ANALYSIS

a. DESCRIPTORS	b. IDENTIFIERS/OPEN ENDED TERMS	c. COSATI Field/Group
*Air pollution		13 B
*Aerosols		07 D
*Filtration		13 K
Filter materials		11 E
*Ceramic fibers		
*Temperature		

18. DISTRIBUTION STATEMENT	19. SECURITY CLASS *(This Report)*	21. NO. OF PAGES
RELEASE TO PUBLIC	UNCLASSIFIED	95
	20. SECURITY CLASS *(This page)*	22. PRICE
	UNCLASSIFIED	

EPA Form 2220-1 (9-73)